A COMPREHENSIVE EVALUATION OF THE EFFECTS OF CLIMATE IN MEPDG PREDICTIONS AND OF MEPDG EICM MODEL USING MNROAD DATA

A THESIS
SUBMITTED TO THE FACULTY OF THE GRADUATE SCHOOL
OF THE UNIVERSITY OF MINNESOTA
BY

LUKE ANTON JOHANNECK

IN PARTIAL FULFILLMENT OF THE REQUIREMENTS
FOR THE DEGREE OF
MASTER OF SCIENCE

ADVISOR: LEV KHAZANOVICH

MARCH 2011

Acknowledgements

I offer my sincere gratitude to my advisor, Professor Lev Khazanovich, for his guidance and financial support during my graduate academic career. I was fortunate to study under a professor with vast wisdom who possesses an exceptional ability to impart his knowledge on others. His contributions extended far beyond my academic pursuit; for this I am humbled and grateful. I wish to express my warm and sincere thanks to Professor Mihai Marasteanu, for admitting me as a graduate student at the University of Minnesota, reviewing my thesis, and for serving on my examination committee. I also extend my gratitude to Professor Douglas Hawkins, for his time and effort reviewing my thesis and for agreeing to serve on my examination committee. A special thanks to Professor Randal Barnes for his contributions regarding data screening.

I wish to thank my many colleagues and friends for their contributions. I would like to specifically acknowledge Derek Tompkins, Kyle Hoegh, Priyam Saxena, Mary Vancura, Peter Bly, Jason Lim, Eyoab Zegeye, and Roberto Piccinin. This thesis and my graduation would not have been possible without them; their help, friendship, and support made my experience at the University of Minnesota a pleasure.

I would like to thank the study partners that sponsored the projects with which I was involved: SHRP 2, which is administered by TRB, under Project R21, Composite Pavements, and an FHWA Transportation Pooled Fund Study, TPF-5(149), Design and Construction Guidelines for Thermally Insulated Concrete Pavements.

Lastly, and most importantly, I wish to express my thanks to my family: to my parents, Roger and Michelle Johanneck, for instilling in me the importance of education; to my siblings, Erika, Thomas, and Patrick Johanneck, for their continuous moral encouragement; and to my beautiful wife, Kristen Johanneck, for encouraging me to pursue my Master's degree, and for her patience and cheerfulness throughout the process.

The love and support they have given me throughout my life is immeasurable. To them, I dedicate this thesis.

Abstract

Although new construction of composite (AC/PCC or PCC/PCC) pavements is not common, a substantial amount of knowledge has been acquired over the past 35 years regarding the materials, design, and construction of composite pavements. The Mechanistic-Empirical Pavement Design Guide (MEPDG) provides useful prediction models, analysis methodologies, and a design procedure that, with further improvements and calibrations, can be made to provide reasonable prediction capabilities for new composite pavements. This thesis investigates the applicability of the MEPDG models for predicting structural responses of composite pavements, with special attention paid to the geographic location of the pavement section, and the temperature distributions predicted by the EICM for a composite pavement.

A section of this thesis examines the effects of climate on pavement performance, and the effect of climate file generation using the MEPDG. This section details the effort to design and test an asphalt-over-concrete (AC/PCC) composite pavement for 610 locations across the United States using the MEPDG version 1.0. While results support the general notion of environmental effects on pavement performance, the performance prediction was found to contain inconsistencies in terms of predicted transverse cracking in the PCC layer. These inconsistencies are attributed to climatic data, and they include the use of stations with incomplete data. It was concluded that the climatic database available to the MEPDG should be cleansed of incomplete or questionable climatic data files to ensure accurate transverse cracking prediction in AC/PCC. Otherwise, the presence of this questionable climatic data can only adversely affect performance prediction.

The other primary focus of this thesis describes research aimed to evaluate modeling of the thermal behavior of concrete and composite pavements by the Enhanced Integrated Climatic Model (EICM), the climate modeling package used in the MEPDG. The study uses temperature data collected at the Minnesota Road Research facility from PCC and

AC/PCC pavements to first investigate benefits of AC overlays on the thermal characteristics of PCC slabs. Furthermore, the study validates EICM predictions of thermal gradients through the slabs and investigates the effect of MEPDG user inputs for thermal conductivity of the PCC. This section examines measured data from MnROAD for AC/PCC pavements and their single-layer PCC counterparts and attempts to explain how similar pavement systems and their thermal characteristics are accounted for in the MEPDG. The research concluded that evaluation of the material thermal inputs should be a part of a process of local calibration and adaptation of the MEPDG.

Also included in this paper is a sensitivity analysis to a wide range of input parameters that might be expected for composite pavements. This includes AC and PCC layer thickness, PCC joint spacing, PCC slab width, and the coefficient of thermal expansion in the PCC layer. Thermal properties of the materials that can affect the temperature distribution, thermal conductivity and heat capacity, are also included in the sensitivity analysis. This thesis concludes that the environmental and material thermal property inputs should be considered with equal importance as traffic, design features, and non-thermal material properties.

Table of Contents

List of Tables

List of Figures

Chapter 1 – Introduction

Although new construction of composite (AC/PCC or PCC/PCC) pavements is not common, a substantial amount of knowledge has been acquired over the past 35 years regarding the materials, design, and construction of composite pavements. The Mechanistic-Empirical Pavement Design Guide provides useful prediction models, analysis methodologies, and a design procedure that, with further improvements and calibrations, can be made to provide reasonable prediction capabilities for new composite pavements.

Climatic factors, such as precipitation, temperature, and freeze-thaw cycles together with the material characteristics of pavement, such as susceptibility to moisture and freeze-thaw damage, layer drainage, and, in the case of composite pavements, infiltration potential of the pavement on which the pavements are constructed, have a major impact on long term pavement performance [1, 2]. Better accounting for these effects will allow pavement engineers to design better, longer-lasting, and more sustainable pavements. However, previous empirical design procedures, such as AASHTO-93, were unable to fully account for these effects.

AASHTO-93 is an empirical pavement design procedure that correlates inputs to serviceability. While the AASHTO procedure has been useful in designing pavements in the past, its empirical nature results in numerous shortcomings that can be addressed by a mechanistic-empirical approach. Though the earliest design models for roadways considered mainly the effects of traffic loading, these models soon evolved to account for the influence of climate and other environmental effects. To that end, modern pavement engineers consider the so-called environmental load to be as critical to design and performance as the volume and type of vehicles traveling a roadway.

The current state-of-the-art in pavement design and performance prediction is the Mechanistic-Empirical Pavement Design Guide (MEPDG) [3]. The MEPDG was

released to the public in 2004, and since that time state and local transportation agencies and other institutions have worked diligently to further understand this significant advance in pavement design and performance prediction. While the incorporation of climate and environment into the MEPDG models is far from comprehensive, the developers of MEPDG took a major step toward accounting for environmental effects through the incorporation of the Enhanced Integrated Climatic Model (EICM). EICM uses hourly climatic data files to predict temperature and moisture profiles, frost heave, and other climate-related phenomena important to MEPDG's analysis of a given pavement system.

Although many aspects of the MEPDG modeling and design inputs have been the subject of a great deal of research, very little of the MEPDG dealing with environmental effects and its impact on pavement performance prediction has been a subject of an in-depth analysis in the past. The goal of this thesis is to fill this gap. The main efforts of this research were a sensitivity analysis of climatic inputs, a sensitivity analysis to EICM material properties, a validation of field temperature data recorded in composite pavements, and a validation of EICM predictions on thermal gradients through the PCC layer of composite pavements.

Chapter 2 – Effect of Climate on MEPDG Predictions for Composite Pavements

Climatic factors affect behavior of all layers in the pavement system. The properties of asphalt are dependent on temperature. At low temperatures, asphalt becomes hard and brittle; at high temperatures asphalt becomes soft and more viscous [4]. As temperature increases, asphalt becomes less elastic and more viscous, and the modulus of the asphalt layer(s) is significantly reduced. Consequently, the pavement cannot support loads as effectively as it can at lower temperatures. At high temperatures, asphalt is prone to rutting, and at extreme low temperatures it is susceptible to thermal cracking [5].

Unlike asphalt, concretes do not see a significant reduction in moduli or flexural strength within the same temperature range. Instead, temperature and moisture gradients in the concrete layer induce stresses and strains by distorting the shape of the slab. If caused by a temperature gradient, these distortions are known as curling; if caused by a moisture gradient, these distortions are known as warping. When these distortions are restrained by dowels, self-weight of the slab, and soil support, stresses and strains are induced [6, 7]. Curling and warping both consist of two parts: a built-in, permanent component, and a transitory component that varies continuously with changing climatic conditions.

Temperature and moisture fluctuations affect the behavior of unbound layers. An increase in moisture content causes soils to become less stiff. As subsurface temperatures drop below the freezing point, moisture in the unbound pavement layers freezes into ice lenses that bind the aggregate particles together. This leads to an increase in the strength and stiffness of the unbound pavement layers and subgrade soil. When the ice lenses thaw, the moisture increase in the soil can lead to weakened support for the pavement structure [8]. Better accounting for these effects will allow pavement engineers to design better, longer-lasting, and more sustainable pavements. However, previous empirical

design procedures, such as AASHTO-93, were unable to fully account for these effects [9].

AASHTO-93 is an empirical pavement design procedure that correlates inputs to serviceability. Two separate design procedures, flexible and rigid, exist for AASHTO-93. The AASHTO-93 procedure was developed at one location and therefore cannot adequately represent climatic effects from locations with different climatic conditions. The procedure has only two environmental inputs: drainage and the seasonal variation of subgrade support. Although these are important effects to consider, alone they are not adequate.

While the AASHTO procedure has been useful in designing pavements in the past, its empirical nature results in numerous shortcomings that can be addressed by a mechanistic-empirical approach. The recently developed MEPDG has addressed this limitation and incorporated a comprehensive Enhanced Integrated Climatic Model as part of the MEPDG design process and design software [10-13]. The MEPDG uses an incremental damage approach, which allows for the consideration of climatic effects and an hourly evaluation of material properties throughout the design life of the pavement.

Since its introduction, numerous studies have been conducted evaluating sensitivity of the MEPDG pavement performance models to the design input parameters [14-17]. The MEPDG framework has been expanding for the modeling of distresses not accounted for in the MEPDG [18]. However, no comprehensive sensitivity study of the effects of climate on pavement performance predictions made by the MEPDG has been conducted. This thesis examines these effects. Included is a brief description of the Enhanced Integrated Climatic Model, a sensitivity study of the effect of climate for 610 stations located across the United States, and analysis at the national, regional, and local levels. The effects of climatic file generation using both station-specific information and virtual station generation through interpolation are also examined.

2.1 Enhanced Integrated Climatic Model

The Enhanced Integrated Climatic Model (EICM) is a one-dimensional coupled heat and moisture flow program that simulates changes in pavement and subgrade characteristics and behavior in conjunction with environmental conditions over numerous years of service [19]. It simulates the upper boundary conditions of a pavement-soil system by generating patterns of rainfall, solar radiation, cloud cover, wind speed, and air temperature [20]. The EICM is comprised of three main components: a climate-materials structural model (CMS Model), a frost-heave and settlement model (CRREL model) developed at the United States Army Cold Regions Research and Engineering Laboratory, and an infiltration-drainage model (ID model) developed at Texas A & M Universities' Texas Transportation Institute [12]. The EICM predicts temperature, resilient modulus adjustment factors, pore water pressure, water content, frost and thaw depths, and frost heave throughout the complete pavement and subgrade profile for the entire design life of the pavement structure [21].

Originally designed for the FHWA in 1989 at Texas A & M University, it was developed as the Integrated Climatic Model (ICM). Larsen and Dempsey revised the original model in 1997, and subsequently released ICM version 2.0 [13]. The EICM was adapted for use in the MEPDG and underwent several major modifications under the NCHRP 1-37A study. Version 2.1 is currently referred to as the Enhanced Integrated Climatic Model (EICM).

The EICM requires information about following five weather-related parameters on an hourly basis throughout the design life of the pavement:

- Air temperature
- Wind speed
- Percent sunshine
- Precipitation

- Relative Humidity

Air temperature, wind speed, and percent sunshine are used to estimate the heat transfer between the road and the atmosphere, as illustrated in Figure 2.1.

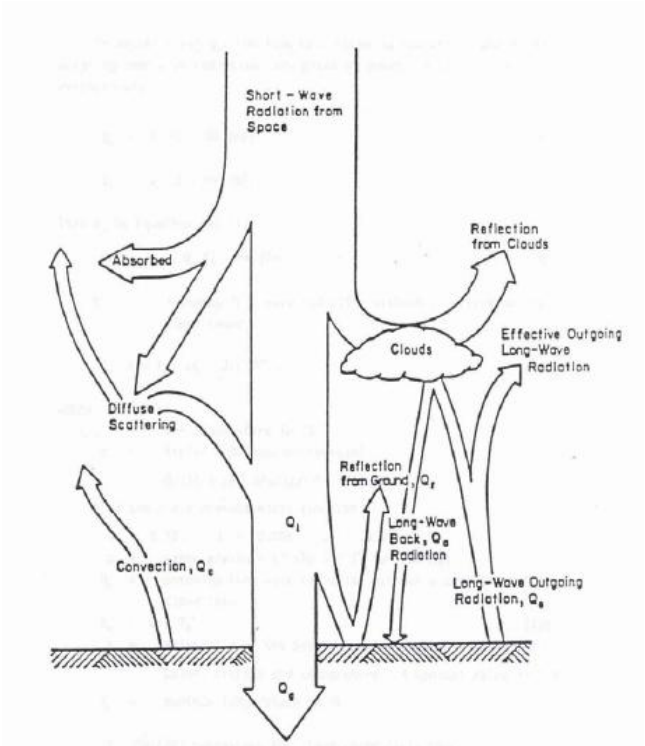

Figure 2.1 - Heat transfer between pavement and air on a sunny day [2]

Temperatures throughout the pavement structure are dominated by atmospheric conditions at the surface. While measuring air temperatures is relatively simple, there is not a direct correspondence between the air temperatures and pavement surface temperatures. To estimate the pavement temperature, the energy balance at the surface used in the CMS model is described in the *Guide for Mechanistic-Empirical Design of New and Rehabilitated Structures* [3]. The Design Guide predicts pavement temperature for every hour based on the following equation.

$$Q_i - Q_r + Q_a - Q_e +/- Q_c +/- Q_h +/- Q_g = 0$$

where,

Q_i = Incoming short wave radiation.

Q_r = Reflected short wave radiation.

Q_a = Incoming long wave radiation.

Q_e = Outgoing long wave radiation.

Q_c = Convective heat transfer.

Q_h = Effects of transpiration, condensation, evaporation, and sublimation.

Q_g = Energy absorbed by the ground.

The convective heat transfer between the pavement and air is affected by the wind speed. Convective heat transfer occurs when the air temperature and pavement surface temperature are not equal. Heat is always transferred from warm to cold, and results in either a gain or loss of heat to or from the pavement. Convection is directly dependent on wind speed, with higher wind speeds resulting in higher convection rates.

Percent sunshine is used in the calculation of heat balance at the pavement surface, and can be thought of as a numerical representation of cloud cover. Incoming shortwave radiation is largely responsible for daytime radiation heating and is dependent on the angle of the sun and the amount of cloud cover. The angle of the sun is dependent on the latitude, date, and time of day.

The EICM does not consider precipitation when determining the surface heat flux boundary conditions. However, precipitation data is used by the EICM to determine the infiltration of moisture in rehabilitated pavements. All precipitation that falls in a month where the average temperature is below 0˚C is assumed to be snow. Relative humidity values are used to model both JPCP and CRCP moisture gradients.

The EICM requires this information on an hourly basis throughout the entire life of the pavement to make temperature and moisture predictions at all depths and throughout the life cycle of the pavement. Because the mechanical properties of materials and distress development are greatly impacted by temperature and moisture, the EICM software provides a distinct advantage over previous procedures [22]. To satisfy the requirements for hourly data on the previously mentioned parameters, the EICM uses climatic data obtained from the National Climatic Data Center (NCDC) for 851 stations located across the United States. Stations exist in all 50 states.

2.2 EICM Climatic Database

The 851 stations available in the design guide have varying amounts of climatic data. The stations with the largest files have 116 months of hourly data. The design guide requires a minimum of 24 months of climatic data for computational purposes [13]. If the design life is longer than the available climatic file, the hourly data is recycled and used again – a pavement designed for 10 years with a 5 year climatic file would use the 5-year climatic data twice; for instance, the climate for years 1 and 6 would be identical.

A station with more climatic data would likely better represent the climatic conditions at that location. Since environmental conditions need to be accounted for over the entire design period of the pavement, data from only 24 months, the minimum amount of climatic data required by the MEPDG, may not represent the climatic conditions well for a particular location. It is widely known that any given year a particular season can be unusually warm or cold, or have above or below average rainfall. If a relatively small number of months of data are used to represent the climate, the data becomes sensitive to outliers, which could be either abnormal weather conditions, or poor data. Even so, 116 months may not be sufficient to represent the climatic conditions at one location. The World Meteorological Organization (WMO) uses periods of 30 consecutive years for

long-term climate averages. The 30-year time period was viewed by WMO as being sufficiently long to address concerns about year-to-year variations [23].

Station locations in the EICM database are well-distributed geographically across the US, and cover a comprehensive range of climates. In this study, to quantify the number of locations existing in different climates, the stations were categorized by freezing index (FI) and Mean Annual Rainfall. The thresholds for the categories were:

- Wet > 25” in rainfall/yr
- Freeze > 200 FI

The number of stations in each category is as follows:

- Dry – No Freeze region: 77 stations
- Dry – Freeze region: 136 stations
- Wet – No Freeze region: 164 stations
- Wet – Freeze region: 233 stations

Hence, the stations are climatologically well-distributed, with a significant number of stations existing in all four categories. This well-distributed, comprehensive climatic data was used to conduct a sensitivity analysis and determine the effect of climate on pavement performance predictions.

2.3 Analysis of Climatic Inputs on MEPDG Predictions

In this study, a single pavement structure was analyzed at a large number of locations. The structure tested at each location was identical, the only variable being the climatic file. A new climatic file (.icm) was generated for a specific station with complete climatic data. Out of the 851 available stations, 610 had complete climatic data. The

MEPDG does not allow a user to generate a new climatc file if the station is missing one or more months of data without using data from nearby stations. This is discussed at length in the section 2.4, *Effect of Climatic File Generation*. The number of months of data in the climatic files is variable – not all complete files have the same number of months of data. The maximum number of months in a climatic file was 116, the minimum number of months in a climatic filed used was 38.

In order to represent all of the effects that climate has on a pavement structure, a composite pavement, Asphalt Concrete over Portland Cement Concrete (AC over PCC), was selected for the MEPDG trial design. Six-hundred ten (610) simulations of composite pavements were conducted. No stations with missing data were used, and no interpolation between stations was done. The following three pavement structures were considered:

- Flexible pavement: 9-in thick AC 58-28PG
- Rigid pavement: 9-in thick PCC, 1.25-in doweled joints
- Composite pavement: 2-in thick AC 58-28PG over 7-in thick JPCP
    - No pre-existing distresses were present in the PCC layer

For all three pavement structures the following inputs were used:

- Design life: 20 years
- Average Annual Daily Truck Traffic (AADTT): 3200
- Joint spacing: 15ft
- Dowels: 1.25-in diameter, 12-in spacing
- Granular Base: 6-in
- Subgrade: A-6
- Water table depth: 5ft
- All other inputs were MEPDG default values

The asphalt binder performance grade is the same at all locations. This report does not suggest that the same performance grade binder should be used at all locations across the country. Rather, the same binder was used to quantify the effects of climate on predicted pavement performance given the same pavement structure.

The analysis of the results of the 610 MEPDG runs were performed in three categories: national, regional, and local. Outputs of interest were: reported transverse cracking, IRI, and AC rutting.

2.3.1 National

The frequency distributions for predicted transverse cracking in the PCC layer, IRI, and AC rutting at the end of the project design life are used below in the discussion of the importance of climate in performance prediction. For each distress, relevant examples from two of the three available projects are used, beginning with the discussion of IRI and Figures 2.2 and 2.3.

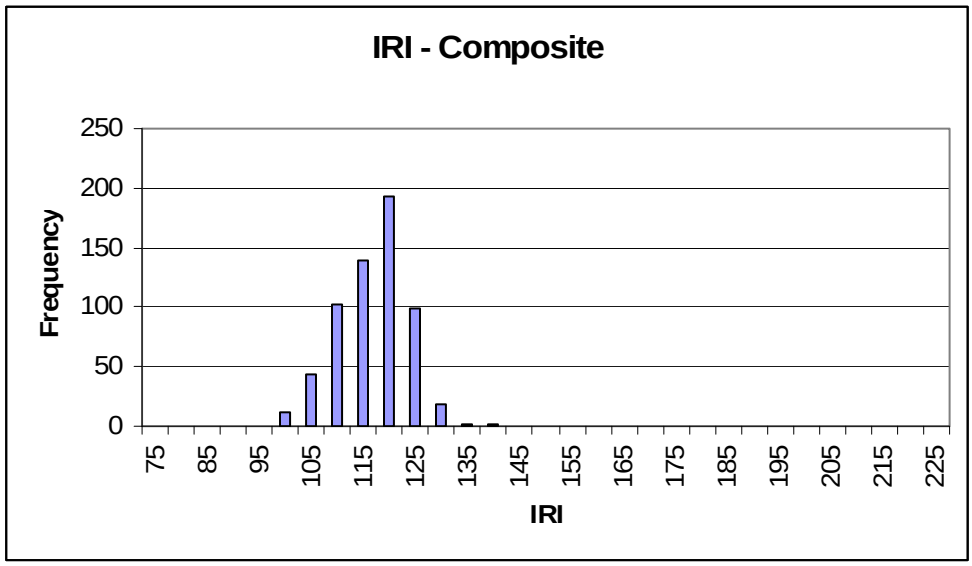

Figure 2.2 - Frequency distribution of predicted IRI values for composite pavement structure.

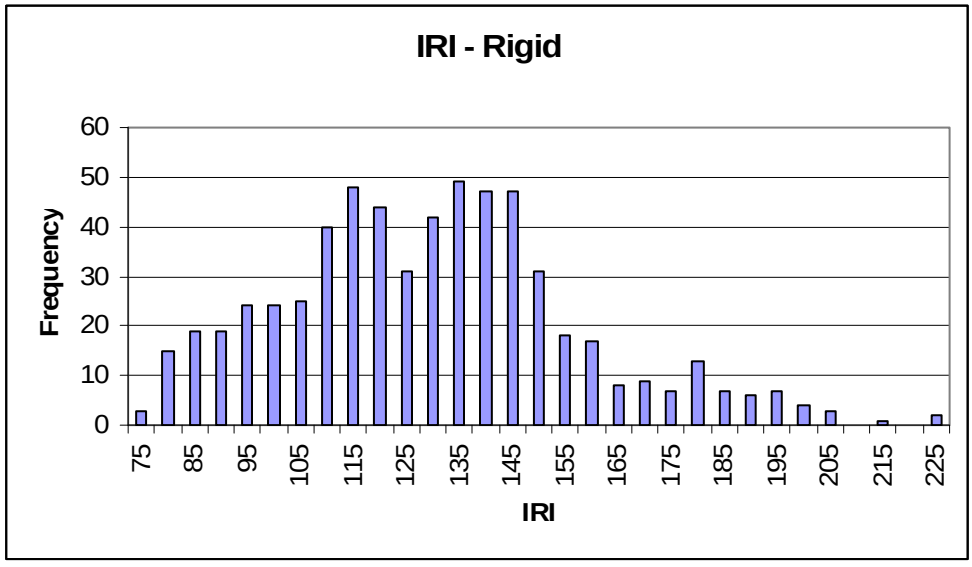

Figure 2.3 - Frequency distribution of predicted IRI values for rigid pavement structure.

The predicted IRI values for the composite structure in Figure 2.2 did not appear to be excessively sensitive to the environmental conditions (note also that the flexible and composite IRI results were very similar). The rigid structure was more sensitive and had more extreme predicted values. A key difference in the reported IRI for AC/PCC and an equivalent single-layer PCC system may lie in the fact that joint faulting is not currently taken into consideration when determining IRI for composite pavements.

Figures 2.4 and 2.5 illustrate the predicted performance in AC rutting of all pavements associated with the 610 climatic files for an AC/PCC pavement and an equivalent single-layer AC system.

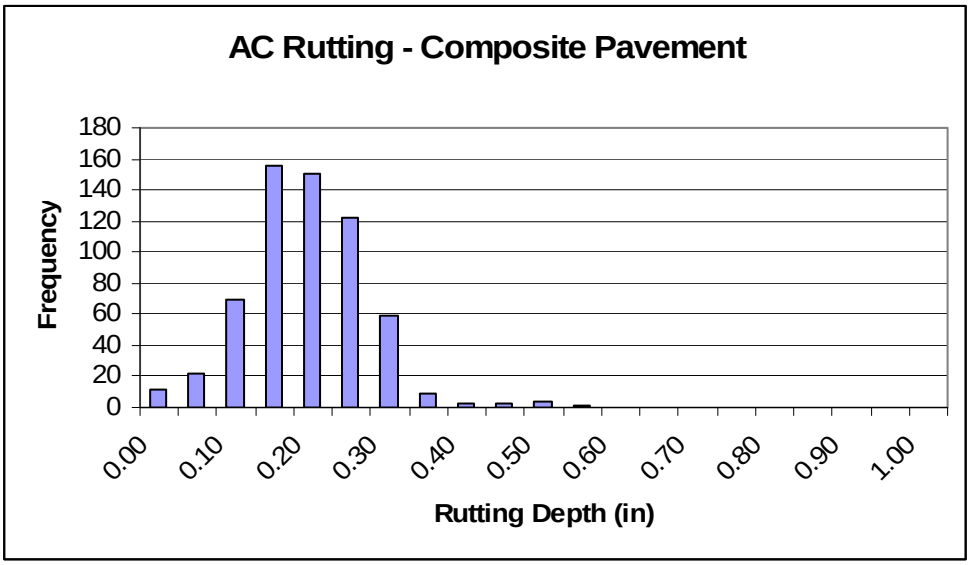

Figure 2.4 - Frequency distribution of predicted rutting values for composite pavement structure.

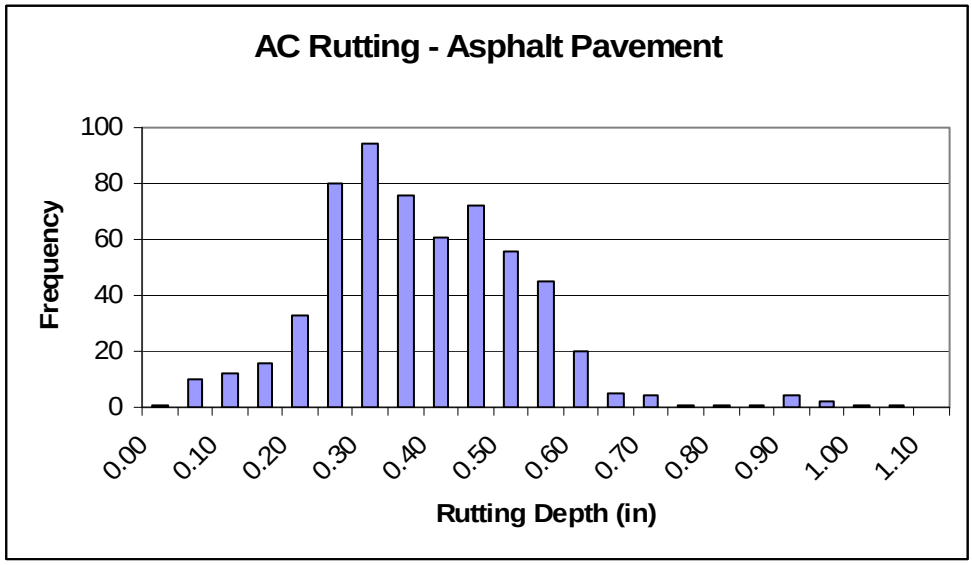

Figure 2.5 - Frequency distribution of predicted rutting values for single layer flexible pavement structure.

As illustrated in Figures 2.4 and 2.5, the composite pavement had less extreme values in AC rutting than the 9" single-layer AC pavement, and the single-layer AC equivalent also experienced more rutting in general. This behavior is attributed largely to the rutting being confined to the AC layer in the composite pavement; that is; no base or subgrade rutting was present due to the PCC layer. The histograms of Figures 2.4 and 2.5 suggest that, according to the MEPDG predictions, an AC/PCC pavement is less sensitive to climate in AC rutting than an equivalent single-layer AC system.

Finally, the analysis of the effect of the location (climate) on predicted transverse PCC cracking for an AC/PCC pavement and an equivalent single-layer PCC system is reported in Figures 2.6 and 2.7.

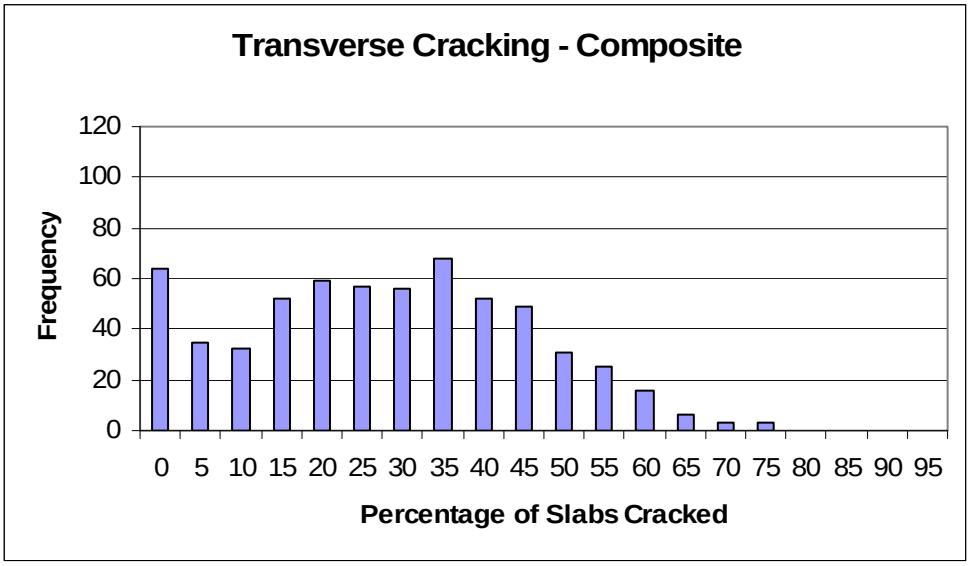

Figure 2.6 - Frequency distribution of predicted transverse cracking values for composite pavement structure.

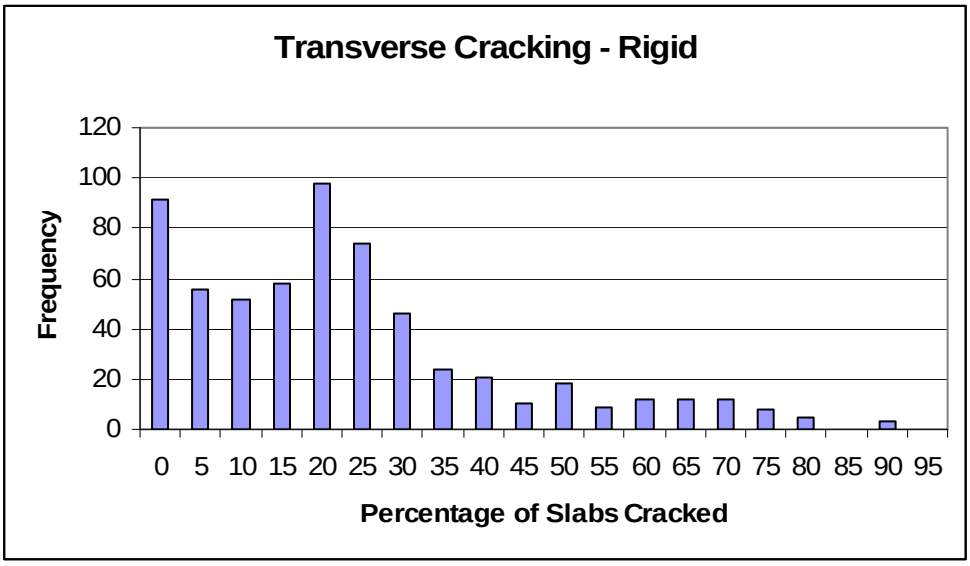

Figure 2.7 - Frequency distribution of predicted transverse cracking values for rigid pavement structure.

Visible in Figures 2.6 and 2.7, the climate has a significant effect on predicted transverse cracking in the PCC layer. This is evident by the wide ranges of values predicted. The minimum values reported for the composite structure were 0.0% in Cold Bay and Bethel,

AK, and the maximum value was 79.1% in Nogales, AZ. The less extreme values predicted for the composite structure are likely a result of the asphalt layer insulating the PCC layer from extreme temperature variations. Based on the analysis at the national level, it was determined that the prediction of transverse cracking in the PCC layer of the composite system was deserving of further attention.

2.3.2 Regional

The predicted cracking output of all 610 stations is organized by the environmental conditions and the predicted cracking percentage, as seen in Table 2.1.

Table 2.1 - Transverse Cracking Percentage in PCC layer of AC/PCC projects, Organized by Environmental Conditions

No. of Stations		Predicted Cracking Percentage			
Climate	**No. of Stations**	**0-15%**	**16-25%**	**26-40%**	**40%<**
Wet – Freeze	233	63	39	93	38
Wet - No Freeze	164	47	14	30	73
Dry – Freeze	136	26	28	42	40
Dry - No Freeze	77	14	13	15	35

In order to better understand the previous table and charts, the values were analyzed by region.

To determine if there were any patterns or tendencies associated with the predicted performance and the region the station was located in, the results were plotted on Google Earth, as seen in Figure 2.8. Each icon represents a station; the icon colors seen in the following figures are associated with the percentage of transverse cracking in the PCC layer:

- Blue: < 16% slabs cracked
- Green: 16% to 25.9% slabs cracked
- Yellow: 26% to 40% slabs cracked
- Red: > 40% slabs cracked

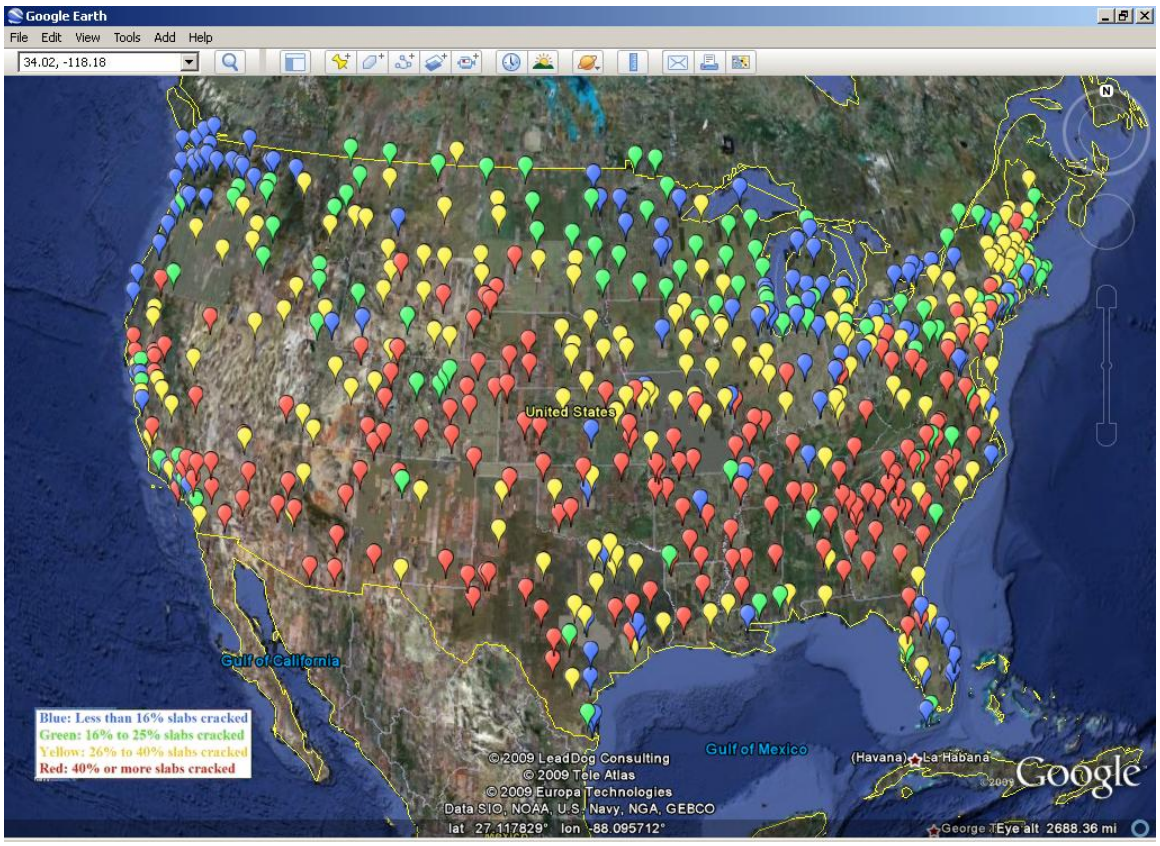

Figure 2.8 - MEPDG locations of AC/PCC projects – icon color determined by transverse cracking percentage.

There are some general trends that are visible when looking at the map of the lower 48 states, such as: higher cracking appears to be at stations with a warmer climate and lower cracking appears at stations with a colder climate. Stations along the coast in California, Florida, Oregon, and Washington exhibit a low predicted cracking percentage. Inland locations across the southern United States generally have a higher predicted cracking percentage, as seen in Figure 2.8 in the states of Arizona, Georgia, and Texas. Stations in

close proximity to other stations do not always have similar predicted values. This was examined in detail in the following section.

2.3.3 Local

It was observed that for some stations in close proximity, there was a high variation in predicted values. In this example, the MEPDG predicted 3.8% cracking using climatic data from LAX International Airport in Los Angeles, CA. The MEPDG predicted 62.7% cracking for Burbank, CA, approximately 18.64 miles away. Given that all other parameters are held constant, this difference of 58.9% should be attributed to the difference in climatic data for these two locations. While there is a difference in elevation of 408 ft. between the two stations, the overall climatic characteristics are otherwise similar. A possible explanation for this anomaly is that the climatic data used was of poor quality, resulting in poor predictions. There are several stations in relatively close proximity, with a wide range of predicted cracking, visible in Figure 2.9.

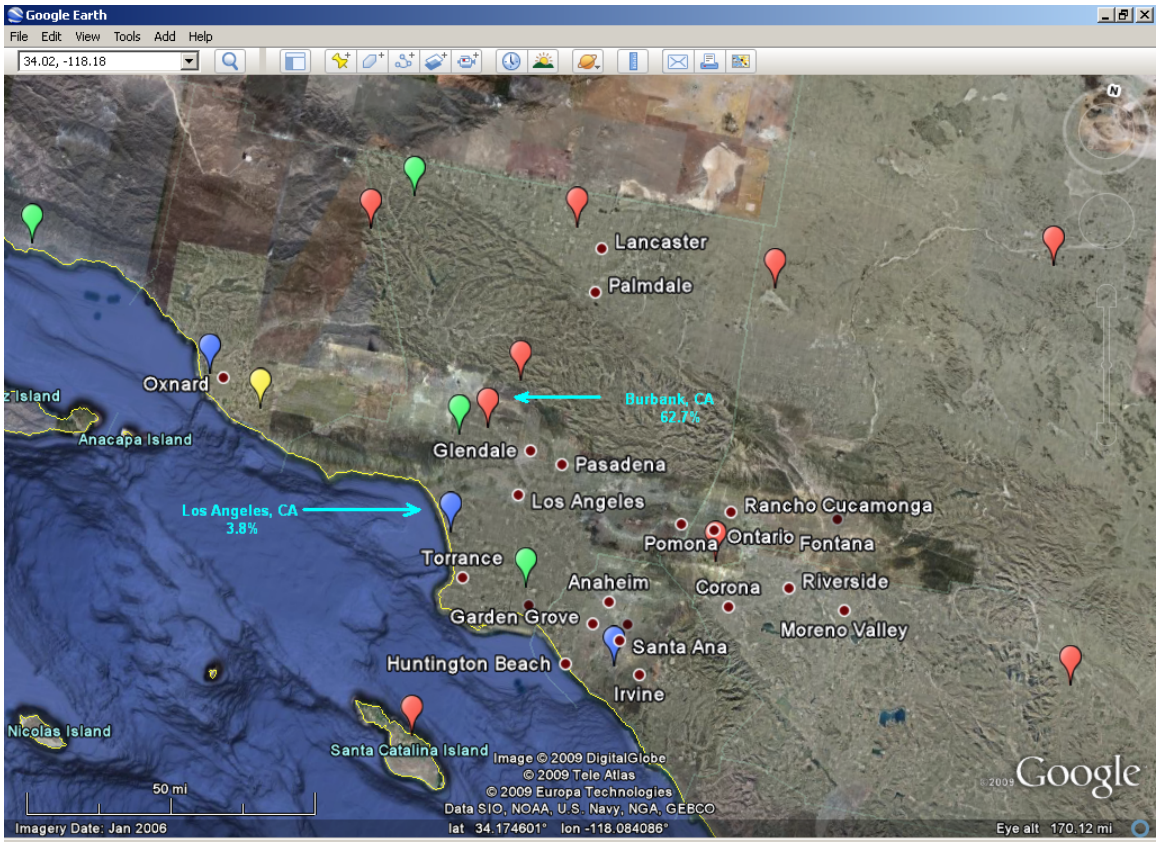

Figure 2.9 - Wide range of predicted cracking in the Los Angeles metropolitan area.

Figure 2.9 illustrates the pattern, or lack thereof, in cracking predictions from the MEPDG. This is visible at several locations throughout the United States. Table 2.3 lists all distresses for each location in Figure 2.9.

Table 2.2 - Predicted Distresses for AC/PCC Projects in Southern California

Location	IRI (in /mi)	Trans-verse Cracking (%)	AC Cracking Top-Down (ft /mile)	AC Cracking Bot-Up (%)	AC Thermal Fracture (ft/mile)	Months of Data	Elev (ft)	Mean Annual Temp (F)	Mean Annual Precip. (in)
Avalon	118.8	47.1	0.0	0.0	169.3	68	1613	59.84	13.32
Burbank	121.3	62.7	0.0	0.0	126.7	94	734	63.44	13.06
Camar-illo	110.9	31.1	0.0	0.0	126.7	77	67	60.23	13.14
Chino	122.5	64.0	0.0	0.0	126.7	95	682	62.16	10.92
Daggett	130.1	61.9	0.2	0.0	126.7	67	1928	67.81	5.72
Lancaster	126.6	59.3	0.1	0.0	126.7	63	2371	62.37	10.19
Long Beach	110.1	23.5	0.0	0.0	126.7	114	37	63.37	12.14
Los Angeles	103.0	3.8	0.0	0.0	126.7	108	326	62.08	14.17
Los Angeles	123.7	66.3	0.0	0.0	126.7	80	185	63.41	14.70
Ontario	116.3	45.5	0.0	0.0	126.7	94	904	63.92	11.17
Oxnard	105.3	14.6	0.0	0.0	126.7	96	68	59.41	10.81
Palm Springs	130.9	67.7	0.2	0.0	126.7	65	447	74.90	3.74
Palmdale	125.8	61.9	0.0	0.0	126.7	95	2562	62.14	6.19
Sandberg	113.4	22.1	0.0	0.0	126.7	116	4519	55.39	13.92
Santa Ana	106.9	14.9	0.0	0.0	126.7	85	52	62.87	10.62
Santa Barbara	109.0	23.0	0.0	0.0	126.7	95	15	58.30	17.01
Santa Monica	108.5	20.6	0.0	0.0	126.7	65	192	61.68	12.94

Generally, stations with higher predicted transverse cracking values also had higher values of predicted rutting. This may be due to the AC layer becoming soft, and unable to support loads effectively, resulting in higher stresses in the PCC layer. However, there was no direct link between the amount of predicted transverse cracking in the PCC layer and predicted AC rutting.

This phenomenon was not unique to southern California. Additional analysis of predicted transverse cracking along the 118-mile length of Long Island in New York was conducted, with the results illustrated in Figure 2.10 and Table 2.3. While some variation is expected, a difference of 32.6% within ten miles (35.7% for Central Park to 3.1% for La Guardia) is difficult to attribute to differences in climate given the proximity of the

weather stations used for these project files. To eliminate this 32.6% difference in predicted cracking, the pavement at Central Park would require an additional 5 to 10 percent in PCC thickness to have performance equivalent to that of the pavement at La Guardia. The performance of these designs at locations within 10 miles of one another is very unusual.

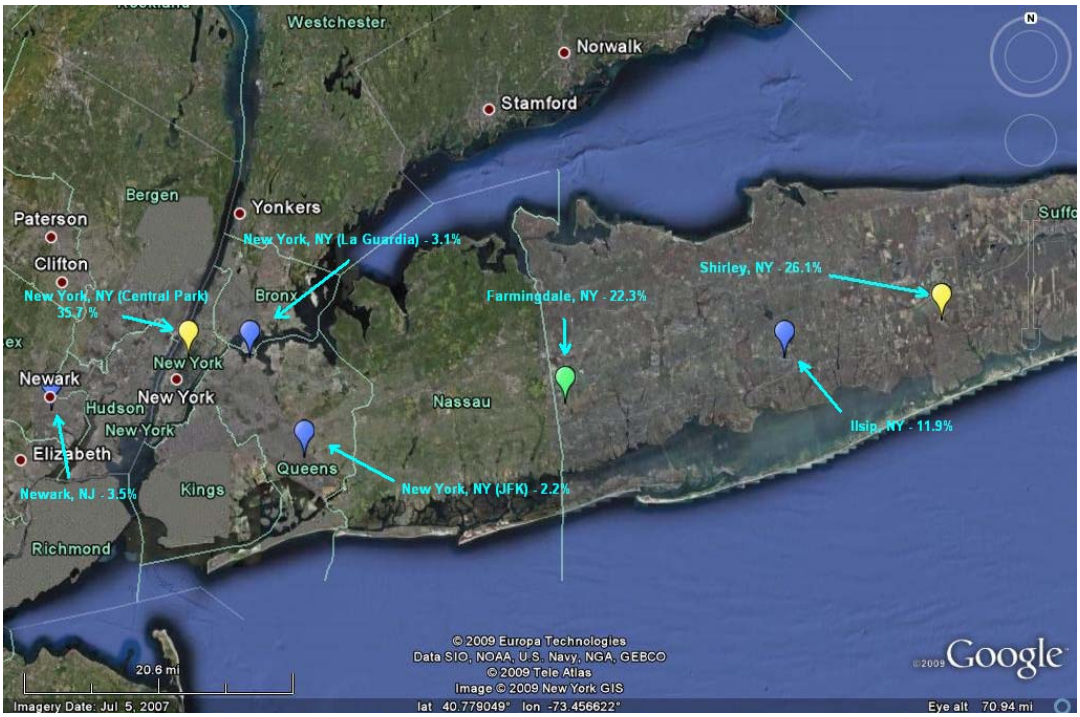

Figure 2.10 - Wide range of predicted cracking in Long Island, New York.

Table 2.3 - Predicted Distresses for Locations near Long Island, New York

Location	IRI (in/mi)	Trans-verse Cracking (%)	AC Cracking Top-Down (ft/mile)	AC Cracking Bot-Up (%)	AC Thermal Fracture (ft/mile)	# of Months of Data	Elev. (ft)	Mean Annual Temp (F)	Mean Annual Precip (in)
Newark, NJ	110.4	3.5	0.0	0.0	126.7	116	28	55.26	42.35
Farmingdale, NY	116.0	22.3	0.0	0.0	126.7	79	74	52.93	42.06
Ilsip, NY	112.5	11.9	0.0	0.0	126.7	79	144	52.36	38.81
New York, NY (Central Park)	121.2	35.7	0.0	0.0	126.7	116	161	55.02	44.43
New York, NY (JFK)	108.9	2.2	0.0	0.0	126.7	116	32	54.15	39.58
New York, NY (La Guardia)	110.1	3.1	0.0	0.0	126.7	116	39	55.63	42.88
Shirley, NY	117.2	26.1	0.0	0.0	126.7	77	71	52.12	41.16

Again, large variation exists in the predicted cracking values among these stations. While there are stations whose extremes act as “outliers” relative to the aggregate data in Tables 2.2 and 2.3 (e.g. mean annual temperature for Palm Springs; elevation for Sandberg; and mean annual precipitation for Palm Springs in the southern California example), by and large the stations represented in Tables 2.2 and 2.3 are very similar climatically, within each table. Hence, the researchers are hesitant to attribute the wide variation in the predicted cracking to climate. Rather, the researchers propose that inconsistencies in climatic data may be responsible for these differences as a hypothesis for future work regarding MEPDG prediction of AC/PCC performance.

2.4 Effect of Climatic File Generation

The MEPDG allows the user to select a design location either with or without an existing weather station. If the location specified does not have a weather station, the EICM will interpolate data from nearby existing stations to create a virtual weather station. The user may select up to six nearby stations for interpolation. If a nearby station has an incomplete climatic file, additional stations may need to be selected. Three different combinations of selected stations are presented in this section.

1. Nearest only – Only the first weather station (out of the six listed) was selected. This station was always closest to the location (latitude, longitude, and elevation) entered.
2. All except nearest – Five out of the six listed weather stations were selected. This selection did not include the first (nearest) weather station.
3. All – All six weather stations were selected.

The effect of the number of weather stations used to generate a climatic file was examined. The output was recorded in terms of predicted transverse cracking in the concrete layer. Design specifications are listed below.

- Composite pavement: 2-in thick AC 58-28PG over 7-in thick JPCP
- Design life: 20 years
- AADTT: 3200
- Joint spacing: 15 ft,
- Dowels: 1.25-in diameter, 12-in spacing
- Granular Base: 6-in
- Subgrade: A-6
- Water table depth: 5ft
- All other inputs were MEPDG default values

The locations were selected away from the mountainous regions of the US and covered a wide geographic area in terms of climate. MEPDG factorials were run for these locations with the same pavement structure as described above. MEPDG defaults were used for inputs other than those listed. The factorials were run for two scenarios for a given location: 1) using the nearest climate station data as the only input or 2) using interpolated climatic data from nearby climatic stations (not including the nearest

station). Table 2.4 provides the percent of cracked slabs after 20 years of the opening of traffic.

This self-consistency test was conducted as a primary evaluation of data quality. If all the weather stations in the MEPDG database were of high quality, then the MEPDG predictions should not depend on the way the interpolated weather station is generated. Table 2.4 illustrates that although the cracking predictions are very close for station climatic data and interpolated climatic data at some locations, for other locations the cracking predictions are dramatically different. The inconsistency in the results indicates that there are some issues with the climatic database, and that the interpolation option may yield inaccurate results depending upon the quality of the climatic data of the nearby locations. A significant difference in predicted cracking indicates that the climatic data is markedly different between the station nearest the location and the surrounding stations. It is known that some of the existing weather stations have incomplete hourly climatic data (.hcd) files. It is thought that the missing weather stations can cause unreliable MEPDG predictions.

Table 2.4 - Predicted Cracking Values

Locations	Lat.	Long.	Elev.	% Cracking after 20 years for weather station	
				Nearby station only	Interpolated climate
Columbus, OH	39.59	-82.53	849	6.4	30.9
Grand Forks, ND	47.57	-97.11	842	9.9	11.0
Fort Wayne, IN	41.01	-85.13	806	12.3	20.1
San Antonio, TX	29.32	-98.28	821	17.5	36.2
Madison, WI	43.08	-89.21	860	18.1	17.1
Oshkosh, WI	43.59	-88.34	816	22.9	19.3
Cedar Rapids, IA	41.53	-91.43	870	24.2	27.1
Ann Arbor, MI	42.13	-83.44	836	27.7	12.2
Joplin, MO	37.09	-94.30	985	37.6	35.9
Lawrence, KS	39.01	-95.13	833	43.0	28.8
Oak Ridge, TN	36.01	-84.14	916	51.5	22.3
Atlanta, GA	33.22	-84.34	837	58.9	19.0

In addition, the researchers conducted a separate local study (in the state of Minnesota) of the effect of climatic file generation, through the corresponding MEPDG interpolation function, on MEPDG predictions of transverse cracking in the PCC layer. The design

specifications for the pavement system under consideration are listed below. The target distress was 20% transverse cracking in the PCC layer at 90% reliability. Inputs other than those listed below were MEPDG default values.

- Composite pavement: 2-in thick AC 58-28PG over 7-in thick JPCP
- Joint spacing: 15 ft,
- Dowels: 1.25-in diameter, 12-in spacing
- Design Life: 20 years
- AADTT: 1300
- Granular Base, 8-in
- Subgrade, A-6
- Water table depth – 5ft
- All other inputs were MEPDG default values

The MEPDG was executed for two different locations in Minnesota (Minneapolis and St. Cloud) approximately 60 miles apart. The climatic files used for these two locations were generated by creating a virtual weather station for each location, using all six available stations for interpolation. A large discrepancy in the transverse cracking predicted for these locations was observed: the MEPDG predicted 20.3% of slabs cracked in Minneapolis, and 60.2% of slabs cracked in St. Cloud. To study the effect further, seven additional locations were selected between Minneapolis and St. Cloud as shown in Figure 2.11. The weather stations used for interpolation for each of the seven additional locations were selected from those made available by the MEPDG, illustrated in Figure 2.12.

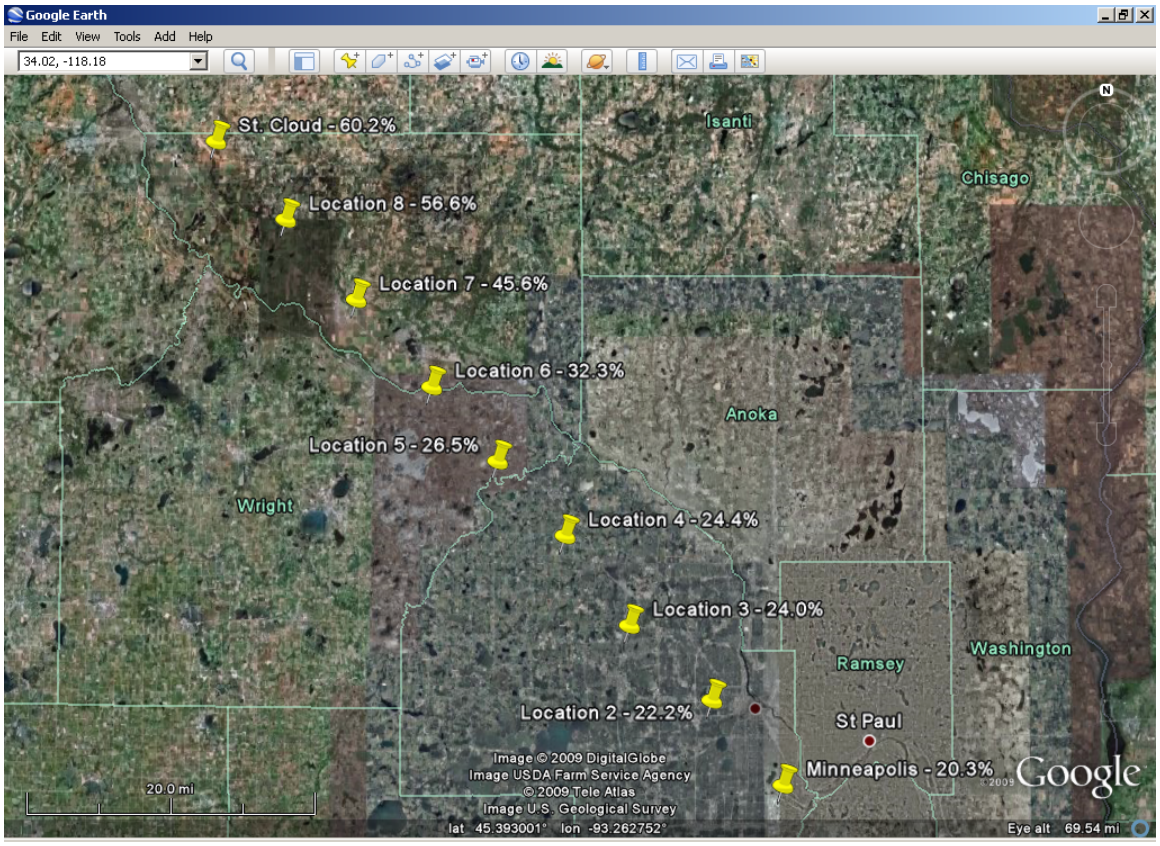

Figure 2.11 - Additional locations selected for MEPDG climate data file interpolation for locations in Minnesota.

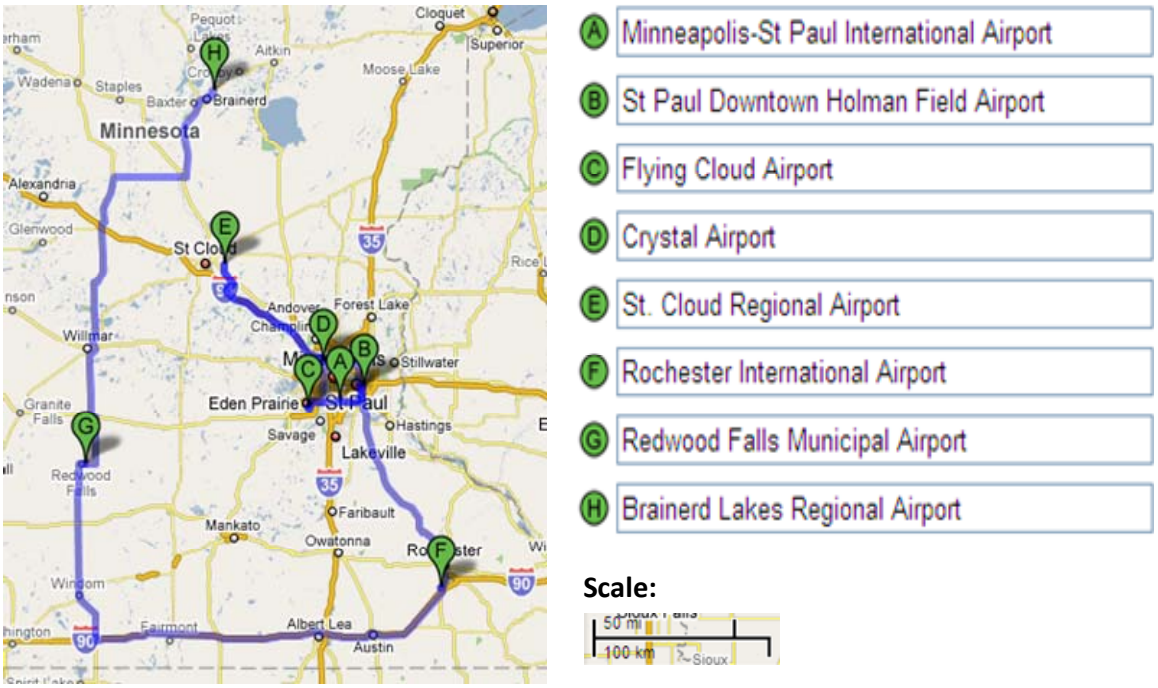

Figure 2.12 - Location of weather stations listed by MEPDG for Minnesota.

Table 2.5 documents the percent slabs cracked for the nine locations after 20 years.

Table 2.5 - Percent Slabs Cracked in AC/PCC Projects for Additional Locations

Locations	Lat.	Long.	% Cracking after 20 years using all weather stations
Minneapolis	44.53	-93.14	20.3
Location 2	44.58	-93.20	22.2
Location 3	45.03	-93.26	24.0
Location 4	45.08	-93.32	24.4
Location 5	45.12	-93.38	26.5
Location 6	45.17	-93.44	32.3
Location 7	45.22	-93.51	45.6
Location 8	45.27	-93.57	56.6
St. Cloud	45.32	-94.03	60.2

Table 2.5 illustrates that in moving along the 60 miles from Minneapolis to St. Cloud, the MEPDG predicts a substantially higher percentage of cracked slabs. Given that the climate from Minneapolis to St. Cloud is not substantially different, this indicates that there is a problem with the St. Cloud station. The largest difference is between Location

6 and Location 7, a difference of 13.3%. It is likely due to the St. Cloud station having missing climatic data. It is already known that the St. Cloud climatic file is missing one month of data, and it is possible that there are other months that may have poor quality or altogether missing data. The other five stations negated some of the effect of the St. Cloud station until the desired location was within an area where the St. Cloud station was weighted heavier. It is thought that the use of weather stations with missing or incomplete climatic data causes unreliable MEPDG predictions. It is recommended that the weather stations with missing data be eliminated from the MEPDG database.

Chapter 3 – EICM Validation

Pavement temperature is not constant in time or through depth. Temperatures throughout the pavement structure are dominated by the atmospheric conditions at the surface. The surface of the pavement is subject to more environmental effects and its temperature will fluctuate more than the temperature at the bottom of the structure.

Factors affecting the top surface temperature of a pavement are: incoming short-wave radiation, reflected short-wave radiation, incoming long-wave radiation, outgoing long-wave radiation, convective heat transfer, condensation, evaporation, sublimation, precipitation; and the temperature of the layer(s) immediately beneath bound layer(s) [3]. The bottom of a Portland Cement Concrete (PCC) slab is affected by the temperature of the layers directly beneath the slab and from energy transferred by conduction from the surface. Although the temperature at the bottom of the slab is ultimately influenced by the conditions at the top surface, it is not directly subjected to the factors that affect the surface temperature. Consequently, pavement temperature is not constant in time and through depth. In particular, temperature variations are especially high at the surface. These variations affect the behavior of rigid pavement structures.

Like almost all other materials, when concrete is heated it expands in size. If the temperature at the top of a concrete slab is unequal to the temperature at the bottom of the slab, different layers of the slab want to expand to varying degrees. The warmer layer attempts to expand more than the cooler layer, but if the shape of the slab is restrained due to foundation support, dowels, tie bars, and self-weight, stresses are induced [6]. These stresses are known as thermal, or curling, stresses. Tensile stresses at the bottom of the PCC layer occur when the top of the slab is warmer than the bottom, which occurs most commonly during diurnal periods; these stresses are known as daytime curling stresses. Tensile stresses at the bottom of the PCC layer are the main cause of transverse cracking in PCC pavements. Thermal stresses can significantly contribute to cracking and

failure of a PCC layer. Therefore, with all other factors equal, a reduction in the temperature difference in the PCC layer would result in lower thermal stresses and less transverse cracking. Thermal stresses can also contribute to other types of distress in rigid pavements. If the bottom of the slab is warmer than the top, the edges of the slab attempt to curl upward. Generally occurring during the night, this nighttime curling stress contributes to joint faulting. Thus, thermal gradients in a PCC pavement are undesirable. Limiting the environmental effects at the top of a PCC slab would reduce the temperature fluctuations at the surface. Because the bottom of the slab does not respond as quickly as the surface does to temperature changes, limiting these effects would reduce thermal gradients.

An asphalt concrete (AC) overlay is a common rehabilitation technique of both asphalt concrete [24] and PCC pavements. Thick AC overlays are used to rehabilitate degrading PCC pavements and improve structural capacity of the existing pavements. Thin AC overlays are used for rehabilitation of structurally sound PCC pavements to cover up surface defects, reduce noise attributed to traffic, and improve ride quality. It has been suggested that the placing of a thin asphalt layer on top of a PCC layer provides an insulating effect [25]. It has been observed by other researchers that an asphalt layer placed on top of an existing PCC pavement can improve pavement performance. While there is a stiffness contribution to the pavement structure from a thin asphalt layer, the improvements in pavement performance suggest that stiffness alone cannot be fully responsible.

This section examines the quality of field data recorded at pavement sections at MnROAD, the thermal insulating effects of AC over PCC overlays, and evaluates the accuracy of predictions of pavement temperature from the MEPDG using MnROAD data. Although thermal stresses can contribute to several types of pavement distresses, transverse cracking is the primary measure of pavement performance used.

3.1 MnROAD Data and Data Analysis

To analyze the EICM performance of predicted temperature distributions, a baseline needs to be established; in this case, measured data served as the benchmark. This section details the efforts of temperature data screening and analysis. Temperature measurements from composite and rigid pavement sections were retrieved, and the data was screened to prevent the use of data with questionable quality, to assure that only data that was representative of the actual conditions was used.

The temperature data used in this section was retrieved from the "mainline" test sections along I-94 at the Minnesota Road Research facility (MnROAD). MnROAD is a full-scale cold-region pavement testing facility constructed in 1994 and administered by the Minnesota Department of Transportation (Mn/DOT). MnROAD is located near Albertville, MN along US Interstate 94. The full-scale testing facilities at MnROAD consist of over 35 sections (or cells) distributed over a west-bound stretch of I-94, a low-volume road loop, and a farm loop. Each of the test cells represents experiments in road research, from pavement materials and design to emerging construction technologies. The test cells are continuously monitored by thousands of live sensors, including more than 1000 thermocouples located at various depths of pavement sections [26]. Data from these sensors are catalogued and maintained in Mn/DOT's database [27].

This study utilized a full year of hourly pavement temperature data, extracted from five test cells along the MnROAD mainline sections, a 3.5-mile stretch of I-94 that carries an average of 26,400 vehicles daily. Those five test cells are three thin concrete cells (113, 213, and 313) and two composite AC-over-PCC cells (106 and 206). The design for each of these cells is illustrated in Figure 3.1.

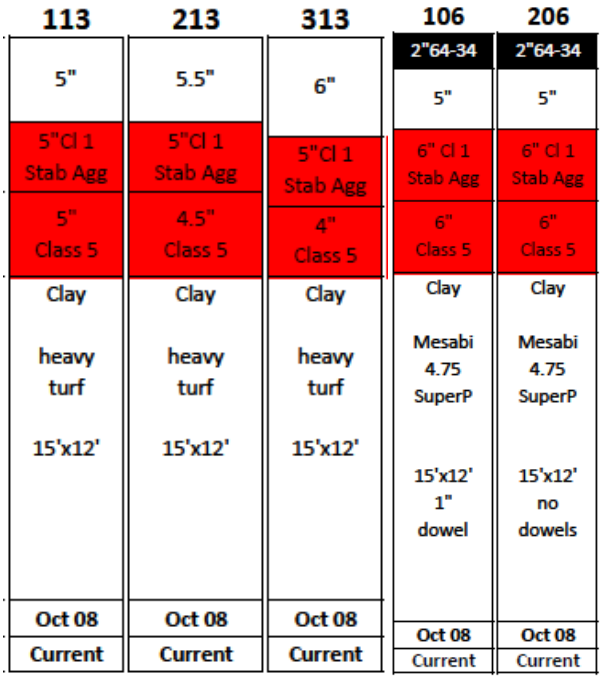

Figure 3.1 - Design cross-section of MnROAD Cells 106, 206, 113, 213, and 313 [27].

As evident from Figure 3.1, the designs of the two sets of test cells are very similar, the main difference between the five cells being the presence of an AC overlay. This difference is at the core of the comparison that uses the data, which is to investigate the difference in thermal readings through overlaid and exposed PCC.

3.1.1 Data Quality Testing

Temperature data from MnROAD was filtered using a program under development by the University of Minnesota, Mn/DOT, and the Minnesota Local Road Research Board for mining of various pavement data [28]. This program subjected the temperature data to different tests to identify missing data, insufficient data for a given day, sensor outliers, data subset outliers, and in so doing flagged suspect data.

Temperature data that appears to be erroneous to the statistical software is flagged. There are fourteen different “flags”, each of which represents a different data test failure. Figure 3.2 is a screen capture of the computer code comments, which define the data flags.

```
In this section we define constants for each of the flags.
%-------------------------------------------------------------------------

% Missing data flags
FLAG_MISSING_DATA            = 1;    % missing data
FLAG_NOT_YET_OPERATIONAL     = 2;    % missing data at the beginning
FLAG_DEACTIVATED             = 3;    % missing data at the end
FLAG_TOO_SPARSE_DAY          = 4;    % not enough data in any day

% Time-series based
FLAG_OUT_OF_RANGE            = 5;    % sensor outliers with annual & diurnal fit
FLAG_NEIGHBORHOOD_OUTLIERS   = 6;    % sensor outliers with local neighborhood
fit
FLAG_LAG_ONE_OUTLIERS        = 7;    % sensor outliers in lag one

% Subset-based flags
FLAG_POINT_EXTREMES          = 8;    % subset outliers, record-by-record
FLAG_DAILY_RANGE             = 9;    % subset daily range outliers, day-by-day
FLAG_DAILY_EXTREMES          = 10;   % subset daily extreme outliers, day-by-day

% Sensor-by-sensor consistency
FLAG_INTERMITTENT_DATA       = 11;   % too many flagged data points around
FLAG_INCONSISTENT_DAY        = 12;   % too small of a fraction of good data,
day-by-day
FLAG_INCONSISTENT_WEEK       = 13;   % too small of a fraction of good data,
week-by-week
FLAG_INCONSISTENT_MONTH      = 14;   % too small of a fraction of good data,
month-by-month
```

Figure 3.2 - Screen capture of computer code comments defining data flags.

This subsection provides a detailed example of the data testing and analysis of temperature data quality from Cells 106 and 206. The intent is to provide the reader a description of the types of quality checks and analysis the data were subject to, not to cover each cell and sensor combination used in the analysis in the later sections in this report.

Temperature data from 48 sensors in cell 106 and 16 sensors in 206 were tested. In some cases, such as cell 106 sensor 28, it is clear there was a problem starting in mid-June 2009, as seen in Figure 3.3; flagged data is green, un-flagged is blue.

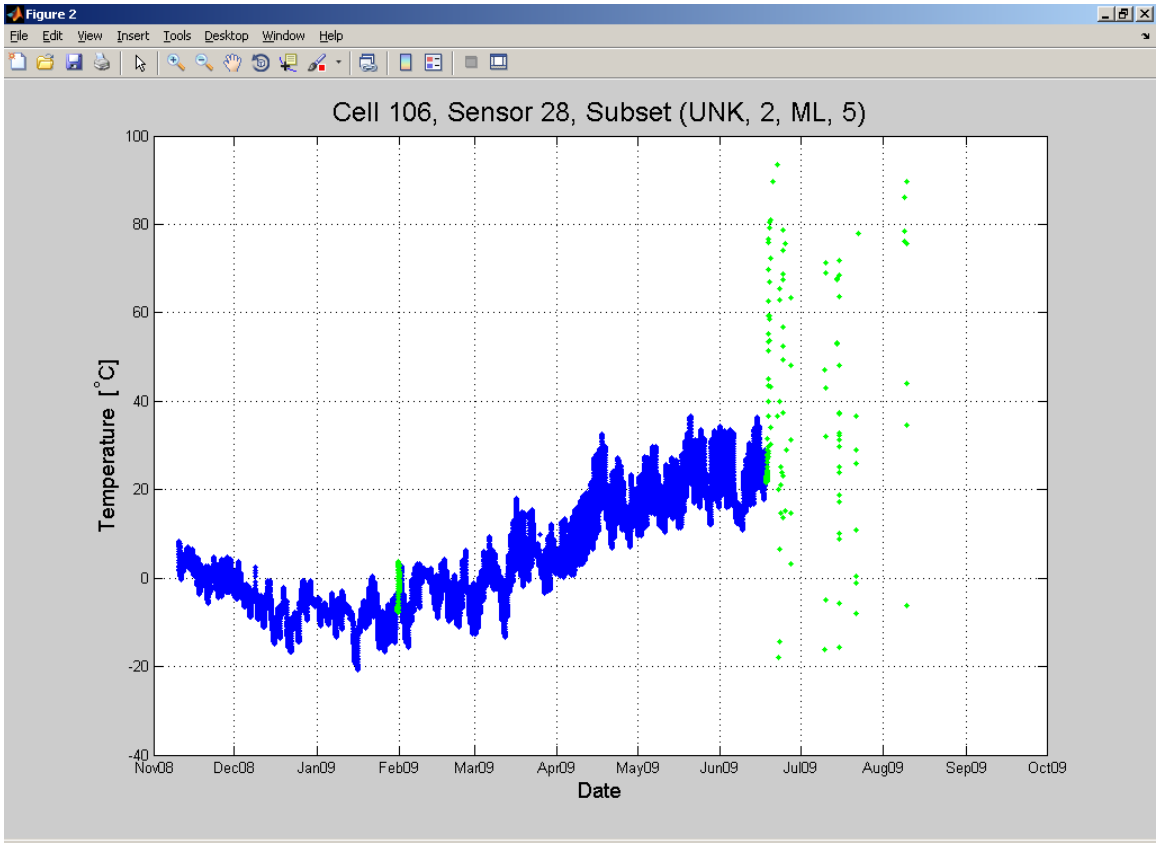

Figure 3.3 - Temperature vs. time plot for Cell 106, sensor 28.

Not all temperature versus time plots are as revealing at first glance. Additionally, small sections of data may be flagged, with the sensor then resuming proper function. Note the period at the end of January 2009 that is flagged in Figure 3.3. A visual inspection does not always provide a clear explanation of what statistical quality check the data is violating. To account for this, another output consists of a plot of flags versus time, visible in Figure 3.4. The flag present is plotted along the ordinate, with time plotted on the abscissa.

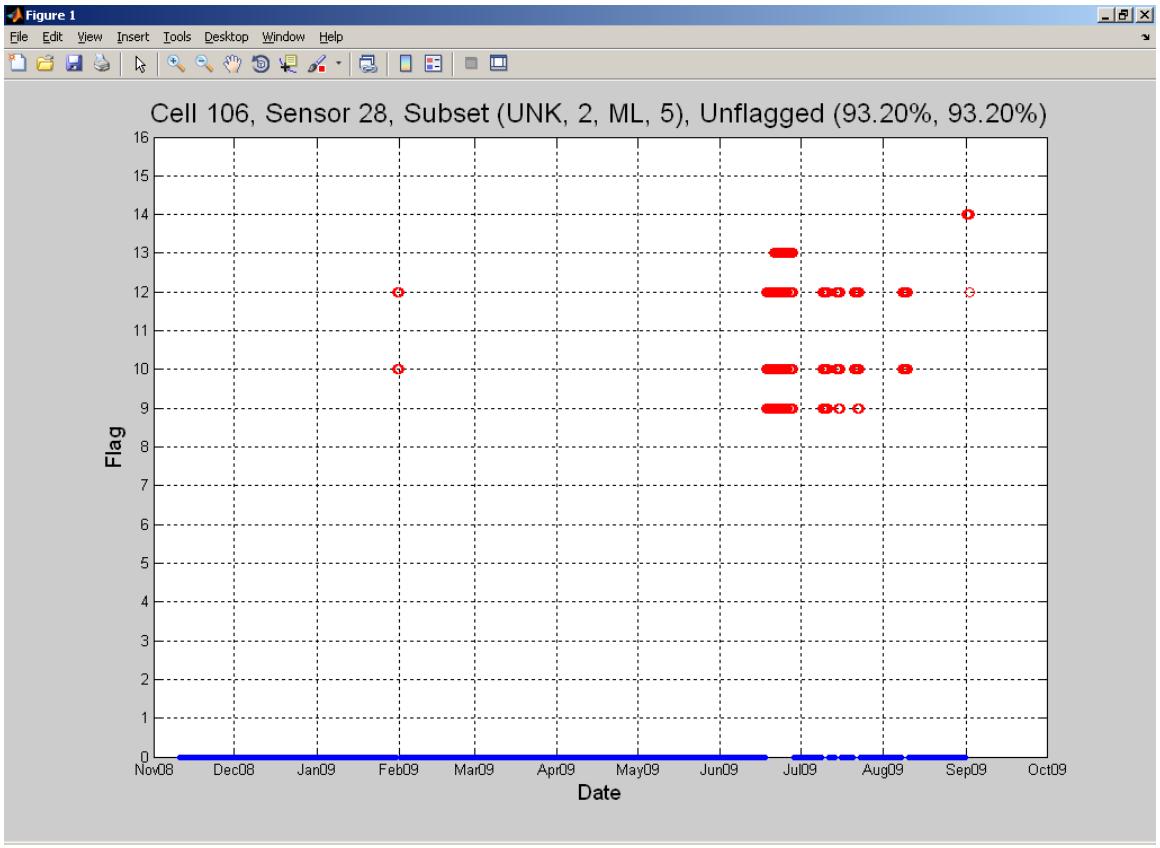

Figure 3.4 - Flag vs. time plot for Cell 106, sensor 28.

The flags present in late January 2009, 10 and 12, indicate that the data has daily extreme outliers, and is inconsistent from day to day, respectively. This means the daily maximum and minimum values are too extreme, and there is too small a fraction of good data, day to day. The data flagged in mid-June has the following flags present: 9 (daily range), 10 (daily extremes), 12 (inconsistent day to day), 13 (inconsistent week to week), 14 (inconsistent month to month). Closer examination of the data flagged in January reveals what is likely the problem, which can be seen in Figure 3.5.

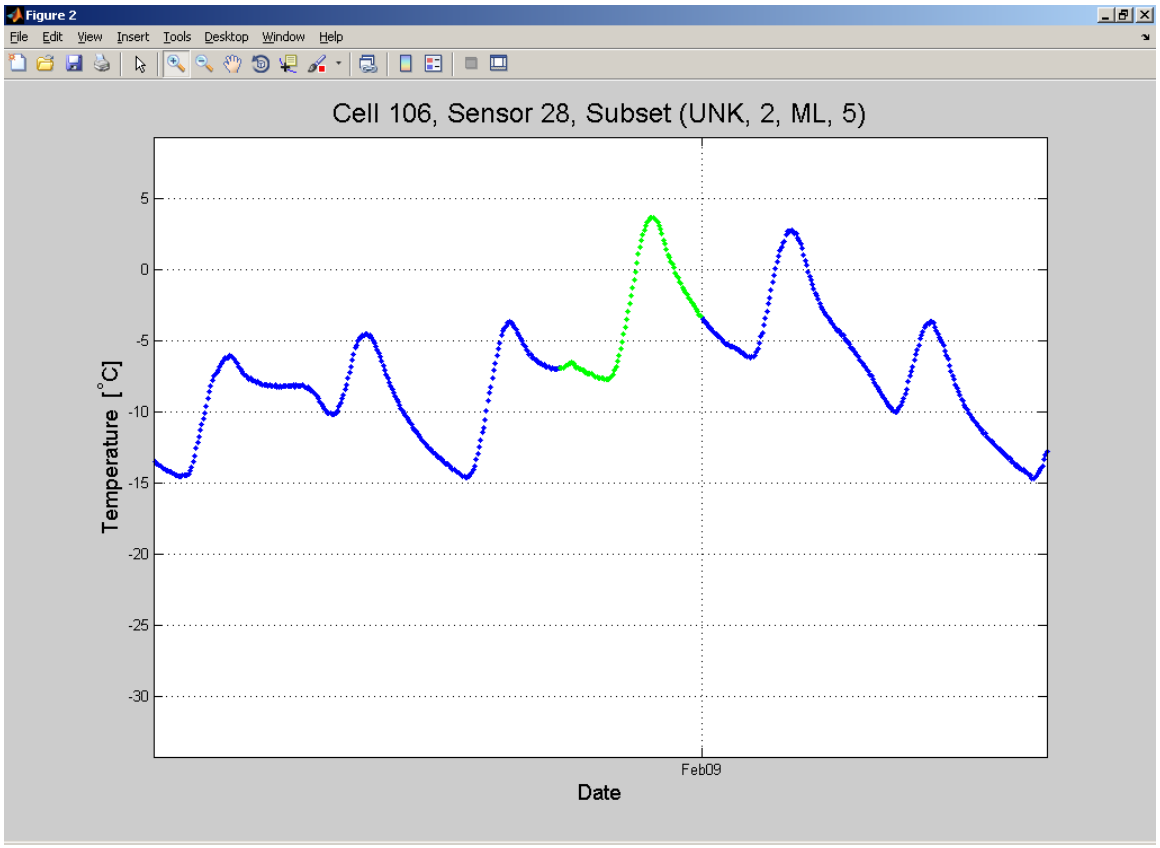

Figure 3.5 - Temperature vs. time plot for Cell 106, sensor 28, January 2009.

The minimum value was "expected" to be lower than what was recorded. This is visible where the data is first flagged, which is plotted in green. Expected values are determined by other observations in the same subset. Sensors in the same subset are located at a similar depth and in a similar material. Even though the data appears acceptable upon initial inspection, especially when observing a large amount of data from longer time period, the software indicated there was a problem.

Figure 3.6 is a close-up of temperature data from the same cell/sensor combination in mid-June. The sensor malfunction is clearly visible.

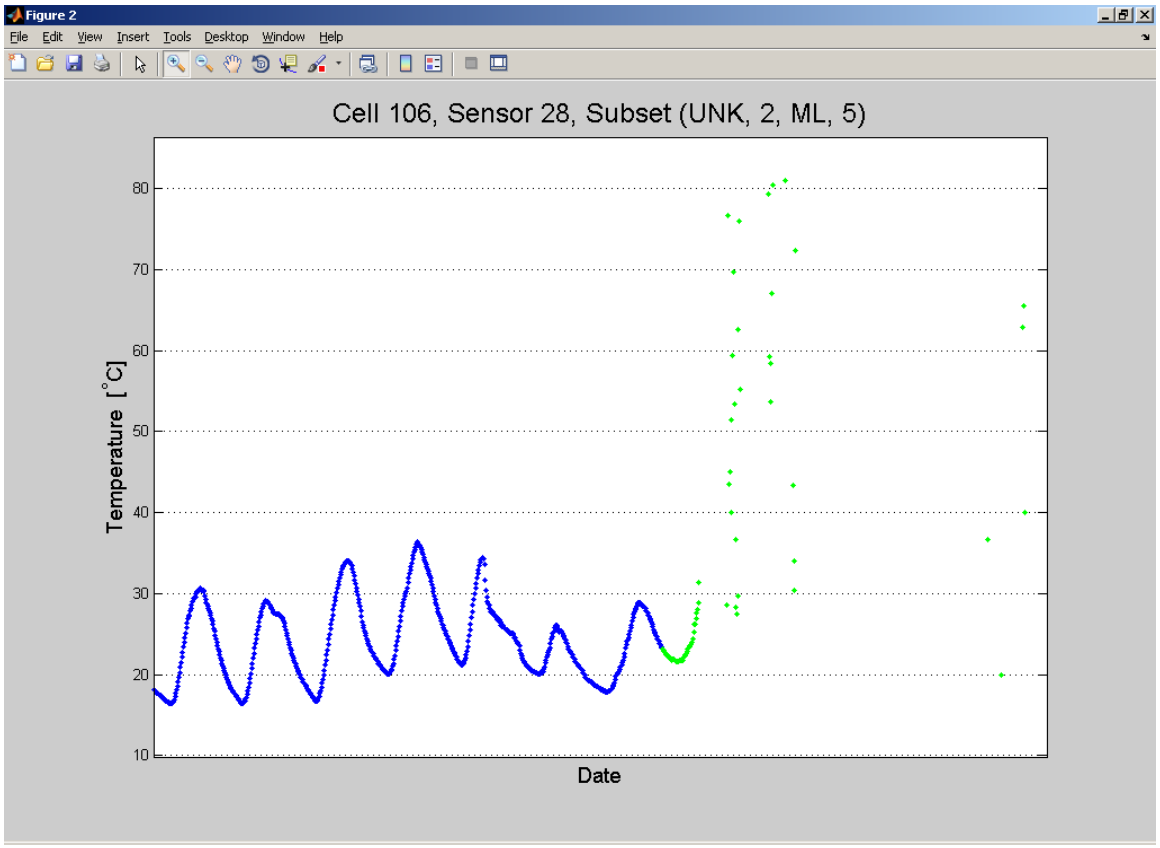

Figure 3.6 - Temperature vs. time plot for Cell 106, sensor 28, June 2009.

Table 3.1 indicates the percentage of un-flagged data for each temperature sensor in cell 106 and cell 206. This information is calculated during the data analysis, and is visible on the flag versus time plots.

It should be noted that in some cases the percentage of un-flagged data might be misleading if that the only output considered in determining the quality of the data retrieved from a specific sensor. That is, flagged data is not necessarily evenly distributed throughout time. For cell 28, 93.20% of the data is un-flagged. Given the high percentage of flagged data, the user may think that entire time period should be discarded. However, inspection of the temperature and flag graphs indicate that the data is reliable and of high quality until about the middle of June 2009.

In summary, temperature data was analyzed from MnROAD test sections 106 and 206. The temperature data was screened, and data that was suspected to be erroneous was flagged. A table indicating the percentage of un-flagged data from each sensor in cell 106 and 206 was presented.

Table 3.1 - Percentage of Un-Flagged Data in MnROAD Cells 106 & 206

Cell	Sensor	Unflagged
106	1	98.95%
106	2	99.29%
106	3	99.29%
106	4	99.29%
106	5	99.29%
106	6	99.29%
106	7	99.63%
106	8	98.28%
106	9	98.61%
106	10	98.95%
106	11	98.95%
106	12	99.29%
106	13	99.29%
106	14	99.29%
106	15	99.63%
106	16	99.29%
106	17	98.28%
106	18	91.51%
106	19	88.80%
106	20	98.28%
106	21	94.22%
106	22	85.42%
106	23	93.54%
106	24	96.92%
106	25	98.28%
106	26	98.28%
106	27	98.28%
106	28	93.20%
106	29	99.29%
106	30	99.63%
106	31	99.63%
106	32	99.63%
106	33	99.63%
106	34	99.63%
106	35	99.63%
106	36	99.63%
106	37	99.63%
106	38	99.63%
106	39	98.28%
106	40	98.61%
106	41	98.61%
106	42	98.61%
106	43	98.61%
106	44	99.29%
106	45	99.63%
106	46	88.13%
106	47	98.95%
106	48	98.61%

Cell	Sensor	Unflagged
206	1	98.07%
206	2	98.83%
206	3	98.83%
206	4	98.07%
206	5	98.07%
206	6	98.07%
206	7	98.07%
206	8	98.07%
206	9	99.21%
206	10	99.21%
206	11	99.21%
206	12	99.21%
206	13	98.83%
206	14	98.83%
206	15	99.21%
206	16	99.21%

3.1.2 Consistency Between Similar Sensor Pairs

The following analysis was performed for Cell 106. The difference in temperature was determined for four similar sensor pairings; the temperature of the uppermost sensor located in the PCC layer of the pavement structure minus the temperature of the bottom sensor in the PCC layer. The four sensor pairings that were analyzed in Cell 106 were: 104 and 106, 112 and 114, 120 and 122, and 128 and 130. These sensors were selected because they were the sensors located closest to the top and bottom of the PCC layer. The pairings were selected because the sensors are similar in that they are located at the same depth, and in the exact same pavement structure, but at varying locations.

Table 3.2 - Depths of Sensor Pairings Located in Cell 106

Cell	Model	Sensor	Depth (ft)	Depth (in)
106	TC	104	0.208	2.496
106	TC	106	0.500	6.000
106	TC	112	0.208	2.496
106	TC	114	0.500	6.000
106	TC	120	0.208	2.496
106	TC	122	0.500	6.000
106	TC	128	0.208	2.496
106	TC	130	0.500	6.000

The depth listed in the Table 3.2 is from the top surface of the pavement. Cell 106 is an AC/PCC composite pavement structure, with a 2-in AC layer on top of a 5-in PCC layer. It is noted that the "top" sensors were located approximately ½ inch below the top surface of the PCC layer, and the "bottom" sensors were located 1 inch above the bottom surface of the PCC layer.

The difference in temperature between the top and bottom sensors were determined for each sensor pairing, and plotted in the histograms found in Figure 3.7.

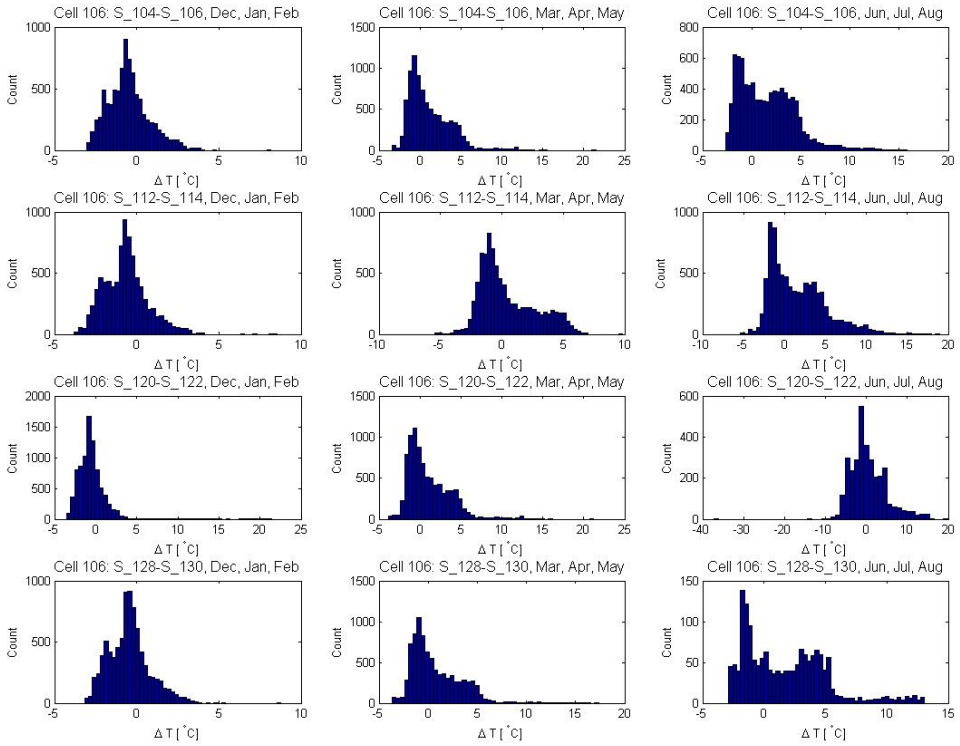

Figure 3.7 - ΔT Histograms for cell 106 sensor pairings, organized vertically by season.

The ΔT "bins," located in Figure 3.7 on the X-axis, indicate the difference in temperature from the top and bottom sensors. The "count" or frequency, located on the Y-axis, represents the number of observations that occurred in each particular bin. The data covered a 9-month time span: December 2008 – August 2009. The histograms are organized in rows according to sensor pairing (e.g. sensors 104 -106 are located in the top row), and in columns according to season (e.g. each histogram in the leftmost column represents data from the months of Dec, Jan, and Feb, and so forth).

Given the organization of the histograms, it is expected that the histograms should look somewhat similar within each column, since the columns are representations of temperature differences from the same season, as observed by different sensor pairings. It is noted that the differences in temperature from the top to the bottom of the PCC layer are more pronounced in the summer months, when the pavement structure is subjected to

longer and more intense periods of incoming solar radiation. During periods where the incoming radiation is less intense (Dec, Jan, Feb) the differences in temperature are not as large.

Temperature data screening was completed for each cell and sensor combination used in the analyses in the following sections of this report. Results varied between sensors, but for the vast majority of the sensors only 1% to 2% of the temperature data was flagged as potentially problematic. No flagged data (i.e. no questionable data) was used in the analysis described in this report. Given the high volume and sometimes suspect nature of temperature data, screening the data allowed the researchers to compare temperature data from the sensors with confidence.

3.1.3 Field Data Analysis

A preliminary analysis of the thermal data meets expectations in many regards. For instance, a natural comparison of an AC-over-PCC pavement with its single-layer counterpart is to investigate the albedo effect. Surface albedo is the effect of color on the degree of absorption of solar radiation and thereby surface temperature. Surfaces with a darker color absorb more incoming solar radiation, and thus have a lower albedo; hence, AC surfaces typically have a lower albedo than that of PCC. Accounting for the albedo effect, one would expect that the surface of the AC-over-PCC pavement would have higher maximum and daytime temperatures than that of a single-layer PCC pavement. This was confirmed with data from MnROAD Cells 106 (AC over PCC) and 213 (JPCP), as illustrated in Figure 3.8.

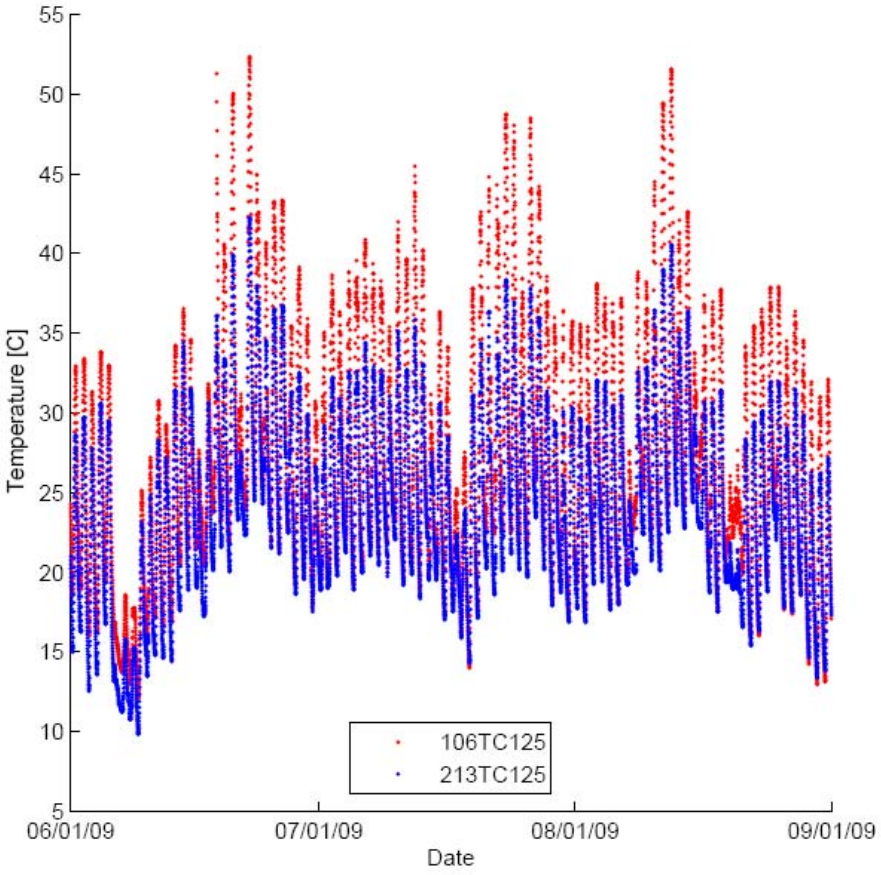

Figure 3.8 - Hourly AC surface temperatures from Cell 106 (in red) and hourly JPCP surface temperatures from Cell 213 (in blue), illustrating the albedo effect.

Note in Figure 3.8 that the AC surface temperatures are clearly higher than the PCC surface temperatures. All other factors being equal, these increased surface temperatures due to albedo lead to greater positive temperature gradients in the AC-PCC system, assuming the temperature near the base is the same in both systems. (Here a positive thermal gradient is one in which the temperature at the surface exceeds that near the base.)

Larger thermal gradients in the composite system do not necessarily create a larger thermal gradient through the PCC slab itself. The presence of the AC overlay may create

an insulating effect, wherein the gradient in the PCC slab in the composite system is less severe than its exposed JPCP counterpart. Figure 3.9 is a plot of temperature differences between the top and bottom of the PCC slabs in an exposed JPCP pavement (Cell 113) and an AC-over-PCC pavement (Cell 106). For Cell 113, the PCC only slab, temperature data is recorded at 0.5 inches and 4 inches from the pavement surface; for Cell 106, the data is taken from thermocouples located at 2.5 inches and 6 inches from the surface. In both cases, the gradient through the PCC slab is described for a vertical distance of 3.5 inches.

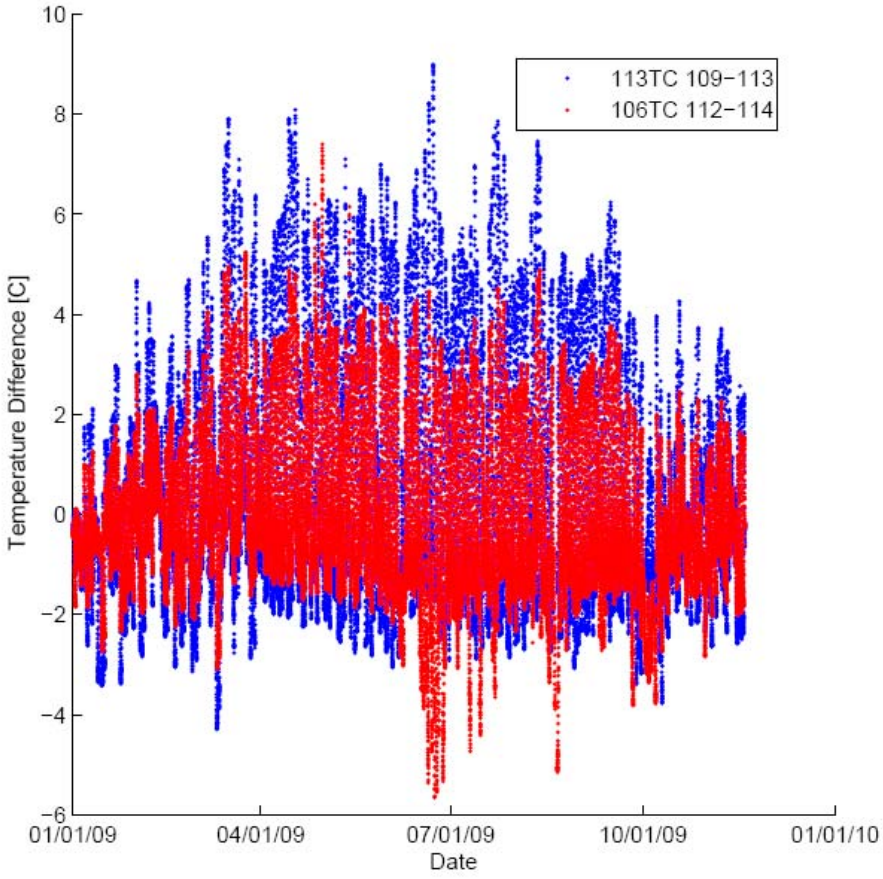

Figure 3.9 - Hourly PCC temperature differences throughout AC-over-PCC (Cell 106 in red) and JPCP (Cell 113 in blue) thicknesses illustrating the insulating effect of an AC overlay.

It is clear in Figure 3.9 that the thermal gradient for the PCC slab is less in magnitude in the AC-PCC composite structure than in the exposed JPCP. This effect can be more closely observed in Figure 3.10, which illustrates hourly detail on the thermal gradient in the same PCC slabs (in Cells 113 and 106) over a two-week span (July 24 – August 7, 2009).

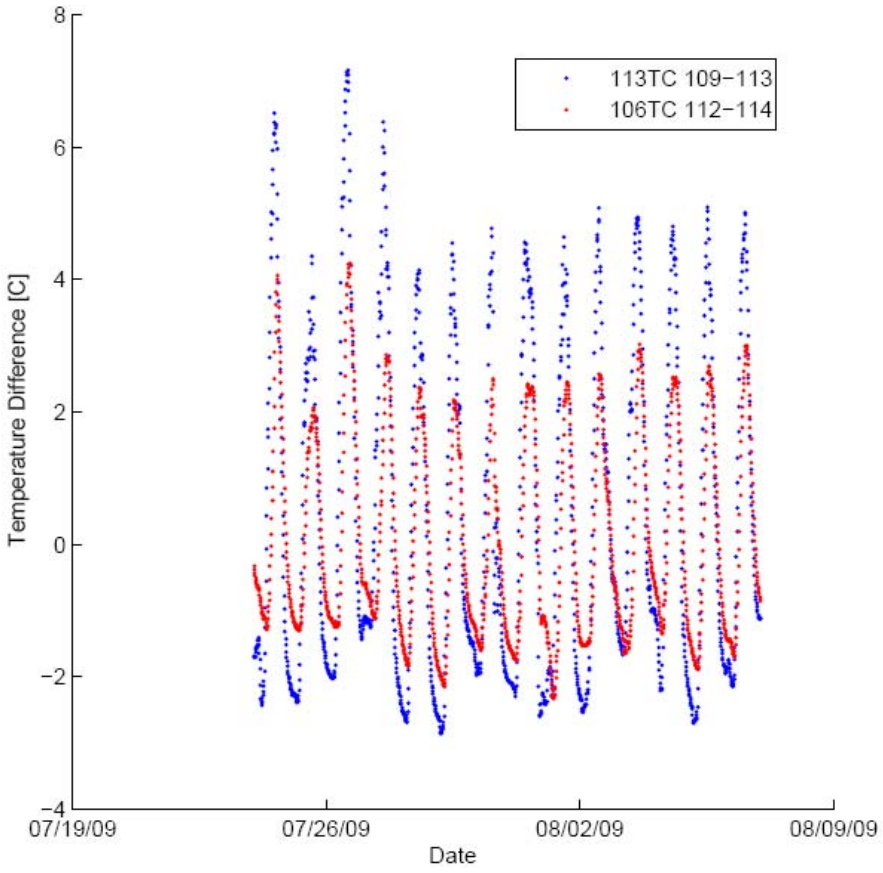

Figure 3.10 - Close detail of hourly temperature differences throughout PCC slab thickness for AC-over-PCC (Cell 106 in red) and JPCP (Cell 113 in blue).

As implied through the use of various time periods for the hourly data of Figures 3.8, 3.9, and, 3.10, the insulating phenomenon of AC overlays will be observed for all seasons. While the effect is more pronounced in the summer months, when solar radiation and

daytime heating are at a maximum, the effect remains observable even in the winter months (which are depicted, in part, in Figure 3.9).

It could be suggested that since the sensors used in Figure 3.9 were located 0.5 inches from the top of the PCC slab – 0.5 inches from the pavement surface for JPCP Cell 113 and 2.5 inches from the pavement surface for AC/PCC Cell 106 – and not at similar absolute depths, the reduction in temperature differences could be attributed to the effect of the sensor location. To disprove this explanation, Figure 3.11 examines thermal gradients for similar overall depths in the composite and JPCP structures. This comparison differs from the comparison visible in Figure 3.9, as both upper locations are at an absolute depth of 2.5 inches below the pavement surface. The bottom locations for this analysis are 5.5 inches for the JPCP Cell 113 and 6 inches for the AC/PCC Cell 106. The vertical distance assumed for each thermal gradient, then, is 3 inches for Cell 113 and 3.5 inches for Cell 106.

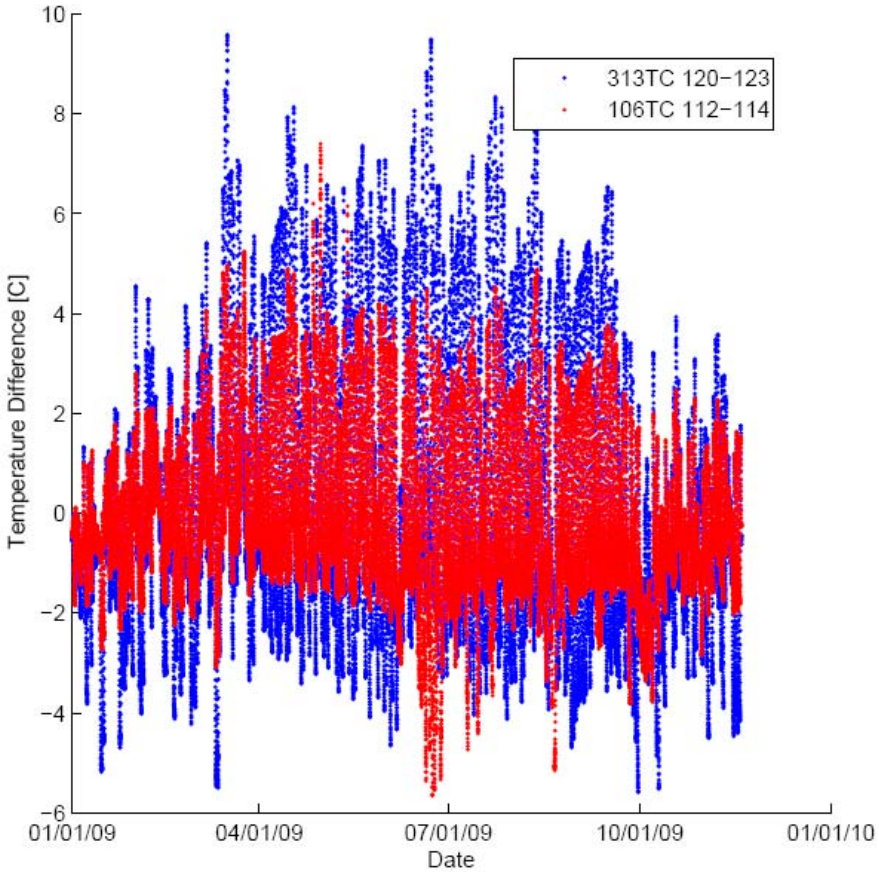

Figure 3.11 - Thermal gradients at similar locations in AC-over-PCC (Cell 106 in red) and JPCP (Cell 313 in blue).

Figure 3.11 confirms the insulating effect of the asphalt layer. The plot shows that even over a slightly greater vertical distance of 0.5 inches, whose additional thickness would increase the magnitude of the thermal gradient, the AC/PCC Cell 106 has markedly lower temperature differences. If temperature distributions were not affected by the asphalt layer, this comparison would yield similar results for each system at the indicated depths. Hence, the insulating effect is not an artifact of selective data analysis.

The EICM simulations also predict that an AC overlay reduces temperature gradients in the PCC layer directly beneath it. Figure 3.12 compares cumulative frequency

distribution of simulated data for July from MEPDG and cumulative frequency distribution of measured data for July from MnROAD. The figure reveals that both the data analysis of temperature data and climatic modeling support the hypothesis that the AC overlay significantly alters the temperature distributions in an underlying PCC slab. Moreover, Figure 3.12 shows good qualitative agreements between the EICM predictions and measured data. In the next section, a quantitative comparison between measured and predicted temperature differences is conducted.

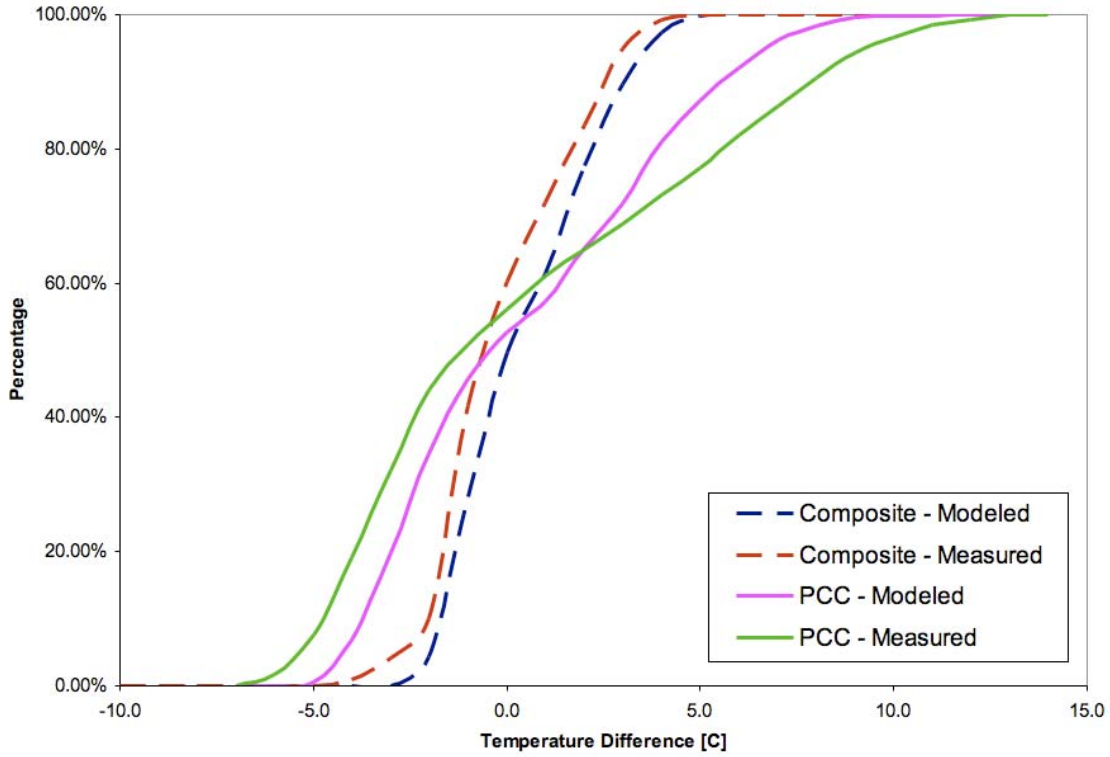

Figure 3.12 - Simulated thermal gradients for AC-over-PCC and JPCP structures and their measured analogues from MnROAD (Cells 106 and 113, respectively).

3.2 MEPDG and EICM Sensitivity to Thermal Conductivity

To date, there have been few large-scale comparisons of EICM predictions for thermal gradients through pavement slabs with measured data. At the outset of this discussion, it should be noted that the EICM uses historical climatic data and does not use or produce climatic forecasts. The climatic data used to produce the modeled data was recorded from a 9 year 8 month period spanning from 1996 – 2006, ending nearly three full years prior to the temperature measurements recorded at MnROAD in 2009. Thus, it is not expected that the modeled data from any single year or an average of years of modeled data will match with the one year of measured data used in this report.

The aim in this discussion of EICM, then, is to better understand the model and the key parameters that drive its predictions for climate – and consequently, predictions of pavement performance for the MEPDG. One parameter that has received little notice given its relative obscurity in pavement research is thermal conductivity. This parameter is often left untouched by pavement engineers; however, as was illustrated earlier for predictions of transverse cracking, its influence can be far reaching in terms of MEPDG performance predictions. The following discussion attempts to characterize the influence of this parameter on EICM predictions.

Measured temperature differences through a JPCP pavement (MnROAD Cell 113) and modeled temperature differences for a JPCP pavement (from MEPDG and EICM) were plotted in a cumulative frequency distribution, visible in Figure 3.13. For this initial comparison, the MEPDG default thermal conductivity value of 1.25 BTU / hr-ft-°F was used for the PCC in the JPCP. The plot represents the temperature distributions for one month (July) of measured data from MnROAD and the minimum and maximum predicted values of seven simulated instances of the same month from seven years of modeled climatic data from EICM/MEPDG.

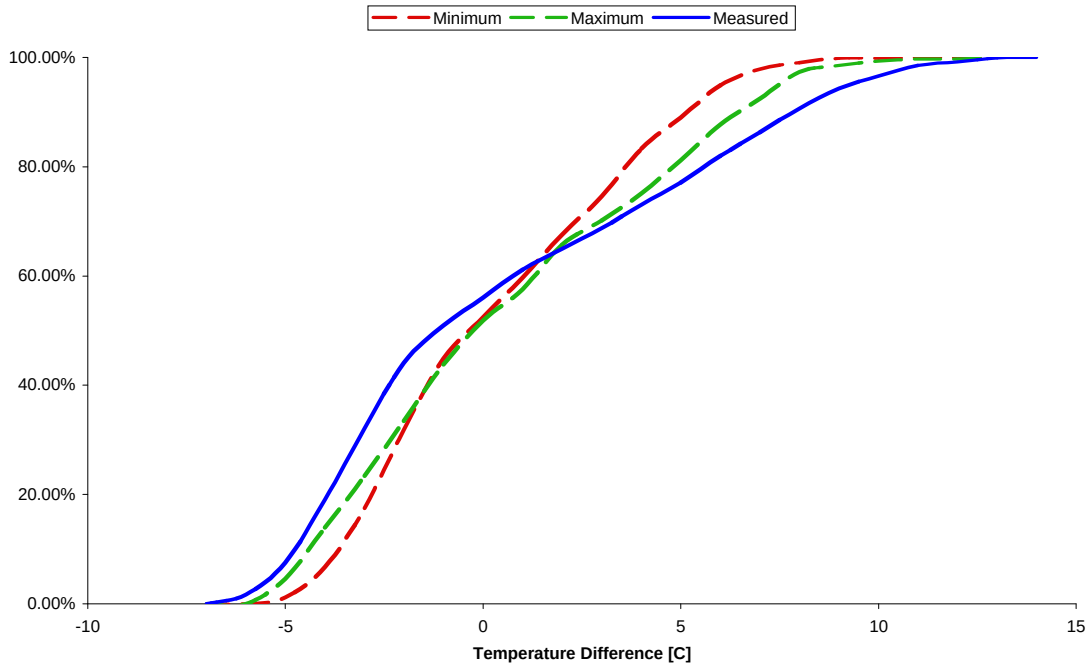

Figure 3.13 - Measured versus modeled cumulative frequency distribution for thermal gradient through JPCP pavement in July with k = 1.25 BTU / hr-ft-°F.

As can be seen from Figure 3.13, the MEPDG underestimates frequencies of positive and negative temperature gradients that were measured in the PCC cells at MnROAD. For example, the EICM predicts that the temperature differences between the top and the bottom surfaces of the PCC should be less than +7°C more than 95% percent of time. The MnROAD measurements show that temperature differences less than +7°C occurred only 86.3% of time, therefore 13.7% of the temperature differences recorded were greater than +7°C. Similarly, the EICM predicts that the temperature difference between the top and the bottom surfaces of the PCC should be less than -3°C 22.4% of time. The MnROAD measurements show that the temperature differences less (more negative) than -3°C occurred 32.3% of the time.

One explanation for this difference is that the reduced temperature differences in the modeled data are, in part, a result of the MEPDG forcing an unnecessarily high value for thermal conductivity on EICM – that is, the thermal conductivity does not match that Cell

113 at MnROAD (the actual value of which is unknown, as it would be for most as-designed or in-field pavements).

The thermal conductivity input was adjusted a lower value of k = 0.94 BTU / hr-ft°F. Figure 3.14 illustrates a similar comparison as Figure 3.13, but with this new value for the thermal conductivity.

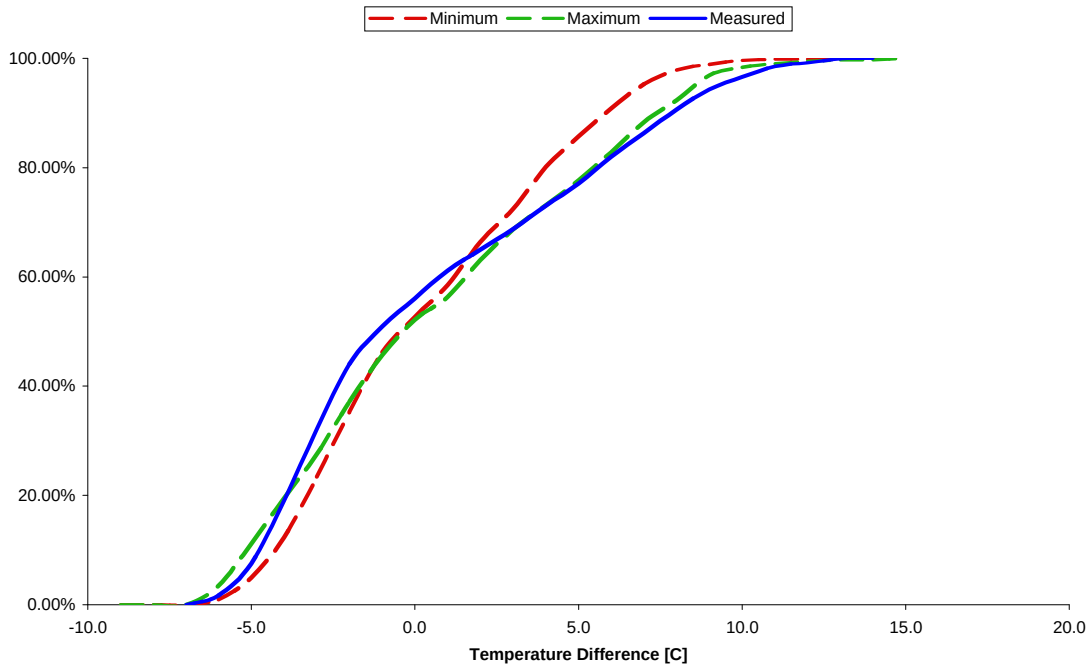

Figure 3.14 - Measured versus modeled cumulative frequency distribution for thermal gradient through JPCP pavement in July with k = 0.94 BTU / hr-ft-°F.

Here it is evident that the lower value of k = 0.94 BTU / hr-ft-°F for the thermal conductivity input brings the simulated minimum and maximum thermal gradients closer to the measured cumulative frequency distribution from MnROAD. To confirm that the adjusted thermal conductivity value improved on the model using the MEPDG default value, other months were examined. Figures 3.15 and 3.16 provide a comparison of modeled and measured data from the month of March for the MEPDG default value for

thermal conductivity and the comparing the default thermal conductivity value and the adjusted value of k = 0.94 BTU / hr-ft-°F.

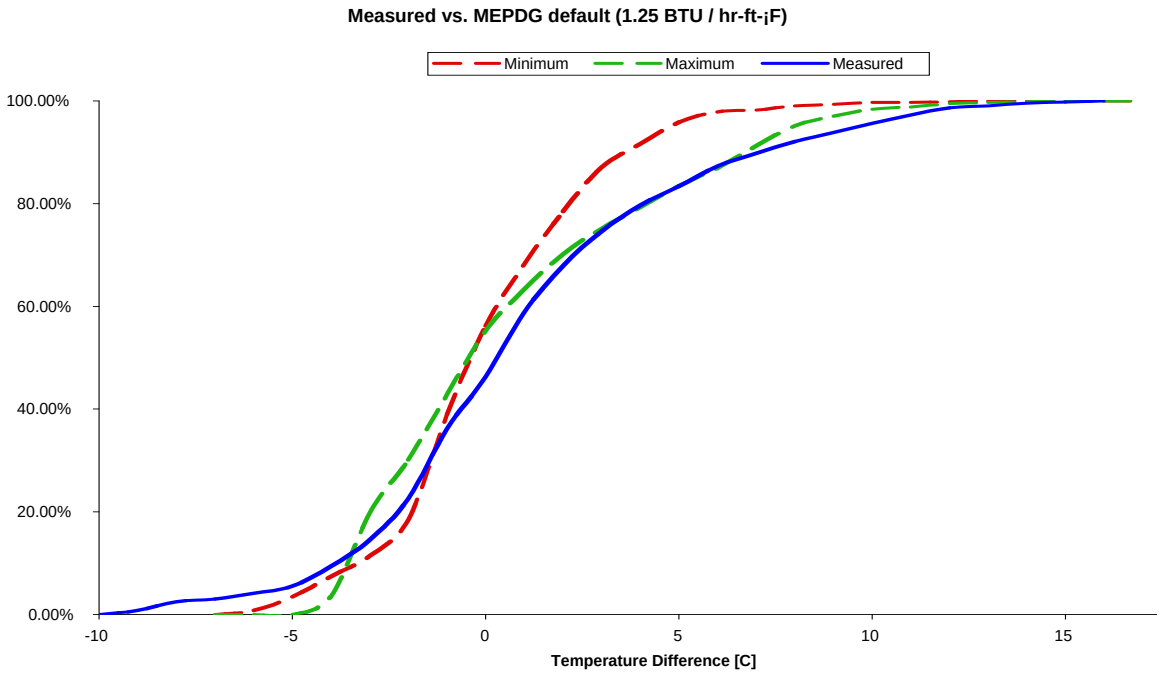

Figure 3.15 - Measured versus modeled cumulative frequency distribution for thermal gradient through JPCP pavement in March with k = 1.25 BTU / hr-ft-°F, which is the MEPDG default value.

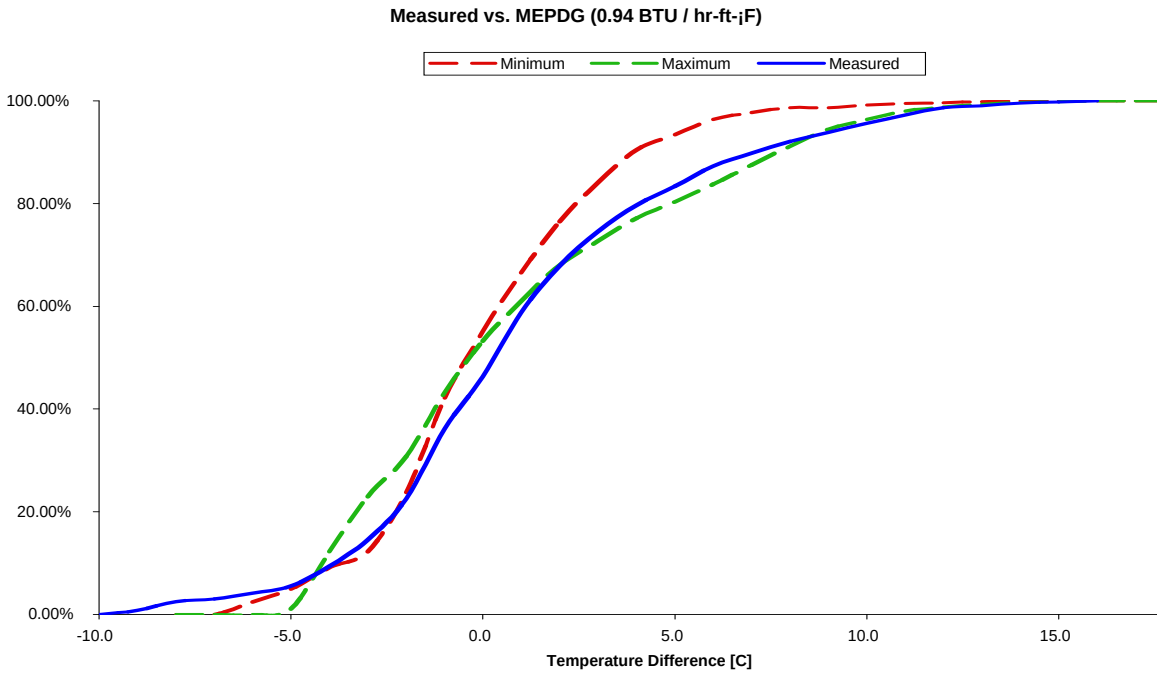

Figure 3.16 - Measured versus modeled cumulative frequency distribution for thermal gradient through JPCP pavement in March with k = 0.94 BTU / hr-ft-°F, the adjusted thermal conductivity value.

The analysis for March and July are indicative of similar analyses performed for other months, all of which suggested that a reduction of the MEPDG default thermal conductivity input value resulted in better agreement between the measured data and the modeled thermal gradients.

Further analysis found, however, that the relationship between measured data and modeled data began to deteriorate for values of thermal conductivity that were less than k = 0.94 BTU / hr-ft-°F. Figure 3.17 is representative of modeled data using a thermal conductivity input less than 0.94 BTU / hr-ft-°F – for this figure, k = 0.85 BTU / hr-ft-°F for the simulated data, which is illustrated against the measured MnROAD data from July once again.

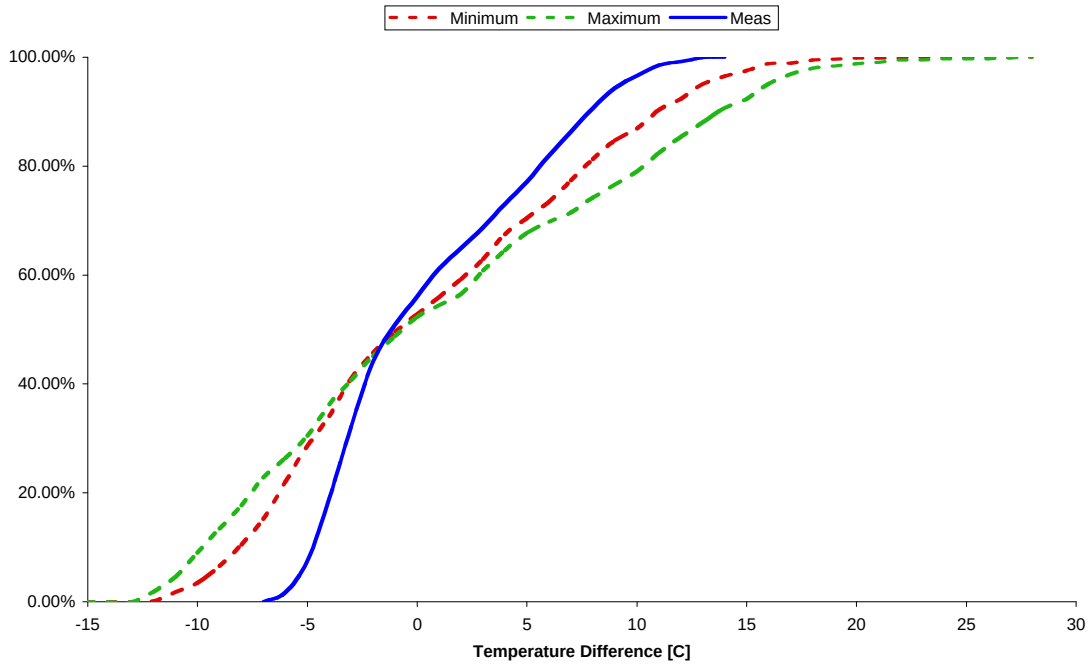

Figure 3.17 - Measured versus modeled cumulative frequency distribution for thermal gradient through JPCP pavement in July with k = 0.85 BTU / hr-ft-°F

As evident in Figure 3.17, the thermal conductivity input value of to 0.85 BTU / hr-ft-°F results in modeled data that is in poor agreement with the measured data collected at MnROAD. This is especially evident by noting the range of values along the abscissa.

Hence, by adjusting the thermal conductivity input to a value lower than the MEPDG default of 1.25 BTU / hr-ft-°F, the predictions of temperature gradients were found to agree better with measured data from MnROAD for PCC slab in JPCP pavements. Furthermore, a range of values were tested for the thermal conductivity, and the analysis found that a value of 0.94 BTU / hr-ft-°F produced the best fit of modeled data to the measured MnROAD data. Although agreement between the measured and modeled data varied from month to month, the value of 0.94 BTU / hr-ft-°F produced the best results for each month. While this value does not produce an exact fit and is not intended to, given the nature of EICM modeling and inherent variability in any data set, the

modifications to the thermal conductivity input represent an improvement over the default value.

It is important to note that only one PCC pavement structure was considered in this analysis. A similar analysis for other MnROAD concrete sections will be conducted in the future.

Chapter 4 – Design Characteristics

4.1 Characterization of Thermal Properties in EICM

Several EICM material properties may affect EICM temperature predictions and subsequently MEPDG performance predictions. This section examines the sensitivity of the EICM and the MEPDG pavement performance predictions to the following EICM thermal property inputs: thermal conductivity and heat capacity.

4.1.1 Thermal Conductivity

The thermal conductivity is a material characteristic indicating the ability of a material to transfer heat. Heat energy is transferred to or from the pavement surface by convection, radiation, or conduction. Materials with a lower rate of thermal conductivity resist the transfer of heat energy. The conduction of heat energy from the surface and from below is what directly influences the temperature in the PCC layer. The MEPDG recommends the following default values of thermal conductivity:

- AC: 0.67 BTU / hr-ft-°F
- PCC: 1.25 BTU / hr-ft-°F

The sensitivity of the thermal conductivity input on predicted transverse cracking was tested for a 2-inch AC over 7-inch PCC composite pavement. Annual Average Daily Truck Traffic was set to 7420, to reach a target of 20% transverse cracking over a 20-year design life using all default values. The location selected was the Minneapolis – St. Paul International Airport; all other MEPDG default values were used. The AC layer thermal conductivity was held constant at the MEPDG default for the model runs where the PCC

thermal conductivity was adjusted, and *vice versa*. Results from the MEPDG model runs are listed in Tables 4.1 and 4.2.

Table 4.1 - Effect of PCC Thermal Conductivity on Transverse Cracking in PCC Layer

Thermal Conductivity - PCC	% Cracking
1.38	15.8
(default) 1.25	20.0
1.13	25.6
1.00	32.0
0.94	35.6
0.85	41.0

Table 4.2 - Effect of AC Thermal Conductivity on Transverse Cracking in PCC Layer

Thermal Conductivity - AC	% Cracking
0.80	30.1
(default) 0.67	20.0
0.54	20.3

It can be observed from Tables 4.1 and 4.2 that the thermal conductivity values can substantially influence the amount of predicted transverse cracking. The differences in the amount of predicted transverse cracking are a result of variations in temperature distributions in the PCC layer. The EICM predicts that the thermal conductivity of the AC and PCC layers are capable of significantly altering the temperature distributions in the PCC layer; consequently, these temperature distributions have a noteworthy effect on predicted pavement performance.

4.1.2 Heat Capacity

Heat capacity is the amount of heat energy required to change the temperature of a material a specified amount. Less energy is required to raise the temperature of a material with a lower heat capacity. The MEPDG recommends the following default values of heat capacity:

- PCC: 0.35 BTU / lb-°F
- AC: 0.23 BTU / lb-°F

Using the same inputs and design employed in the thermal conductivity analysis, the sensitivity of the heat capacity input on predicted transverse cracking was examined. The results are listed in Tables 4.3 and 4.4.

Table 4.3 - Effect of PCC Heat Capacity on Transverse Cracking in PCC Layer

Heat Capacity - PCC	% Cracking
0.35	12.2
(default) 0.28	20.0
0.21	32.1

Table 4.4 - Effect of AC Heat Capacity on Transverse Cracking in PCC Layer

Heat Capacity - AC	% Cracking
0.29	15.2
(default) 0.23	20.0
0.17	25.8

As can be observed in tables 4.3 and 4.4, an increase in heat capacity results in a reduction of predicted transverse cracking predicted by the MEPDG. This was true for both the AC and PCC layer in the structure. This is attributed to the material being able to contain more heat energy without changing temperature, which resulted in a lower thermal gradient in the pavement structure as compared to a material with a lower heat capacity. A change in heat capacity in the PCC layer had a larger effect on predicted transverse cracking when compared to a similar change in the AC layer.

4.1.3 Coefficient of Thermal Expansion

A third PCC thermal property input is provided by the MEPDG, namely, the *coefficient of thermal expansion*, which is the change in volume of a substance per unit temperature. Although it is an important parameter to consider when predicting rigid pavement performance, the coefficient of thermal expansion does not affect the temperature distribution throughout the pavement structure. Rather, the temperature distribution influences how much of an effect the coefficient of thermal expansion has. Large temperature variations in the PCC layer will result in greater expansion and contraction, which may result in thermal stresses and cracking. The sensitivity to the coefficient of thermal expansion of the PCC layer was examined for both a PCC and AC/PCC structure, and the results are listed in Tables 4.5 and 4.6. The MEPDG recommends the following default values for the coefficient of thermal expansion:

- PCC: 5.5 per °F * 10^{-6}

Table 4.5 - Effect of the Coefficient of Thermal Expansion in the PCC Layer on Predicted Pavement Performance of an AC/PCC Pavement

Coefficient of Thermal Expansion (PCC)	% Cracking
4.125	13.3
5.5	20.0
6.875	30.7

Table 4.6 - Effect of the Coefficient of Thermal Expansion in the PCC Layer on Predicted Pavement Performance of a PCC Pavement

Coefficient of Thermal Expansion (PCC)	% Cracking
4.125	3.3
5.5	20.0
6.875	78.7

As expected, a decrease in the coefficient of thermal expansion of the PCC layer resulted in lower predicted transverse cracking values from the MEPDG. It is important to note

that the composite AC/PCC structure was far less sensitive than the PCC-only rigid pavement to differences in the coefficient of thermal expansion of the PCC layer. This appears to be due to the insulating effect of the AC layer. When the PCC layer is exposed it is subjected to greater temperature fluctuations; greater fluctuations and extreme temperatures exposed to a PCC layer with a high coefficient of thermal expansion results in higher cracking.

4.2 Characterization of Design Features

4.2.1 AC & PCC Layer Thickness

In this sub-section, a sensitivity analysis of layer thicknesses of an AC/PCC pavement is conducted. The effect of PCC layer thickness on a composite structure was evaluated at two different AC thicknesses. The following inputs were common to all cases examined for the sensitivity analyses in this section:

- Design life: 20 years
- Climatic input file: Minneapolis – St. Paul, MN Int'l Airport (MSP)
- Joint spacing: 15ft
- Dowels: 1-in diameter, 12-in spacing
- Granular Base: A-1-a, 6-in
- Subgrade: A-6
- Water table depth: 5ft
- All other inputs were MEPDG default values

The Annual Average Daily Truck Traffic (AADTT) was set for a target of 20% cracked slabs in the PCC layer for two composite structures: a 2-in AC over 7-in PCC, and a 3-in AC over 6-in PCC structure. In each case, the AC thickness was held constant, and the

PCC was adjusted +/- 2-in at 1-in increments. The results are listed in Tables 4.7 and 4.8 and Figures 4.1 and 4.2.

Table 4.7 - Effect of PCC Thickness for an AC/PCC Composite Pavement with a 2-in AC Layer

AC Thickness	PCC Thickness	Traffic	% Cracking
2	5	7420	99.8
2	6	7420	89.3
2	7	7420	20.0
2	8	7420	0.2
2	9	7420	0.0

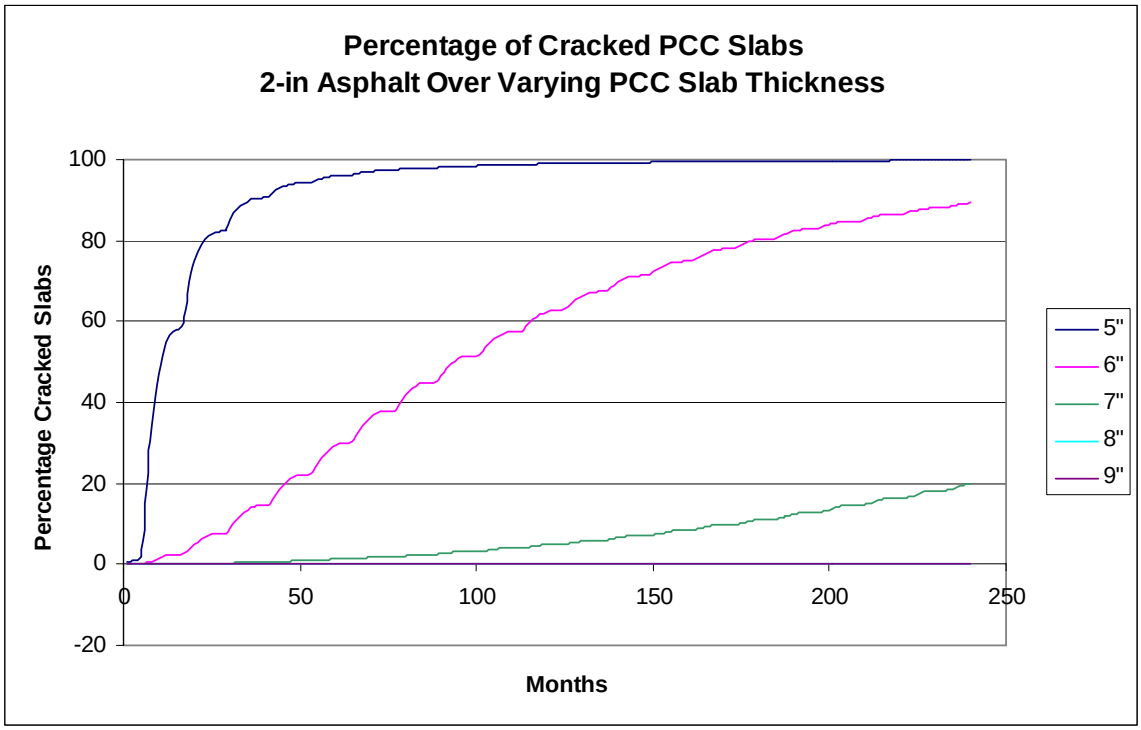

Figure 4.1 - Effect of PCC thickness for an AC/PCC composite pavement with 2-in AC layer.

Table 4.8 - Effect of PCC Thickness for an AC/PCC Composite Pavement with a 3-in AC Layer

AC Thickness	PCC Thickness	Traffic	% Cracking
3	4	4325	99.9
3	5	4325	96.9
3	6	4325	20.0
3	7	4325	0.3
3	8	4325	0.0

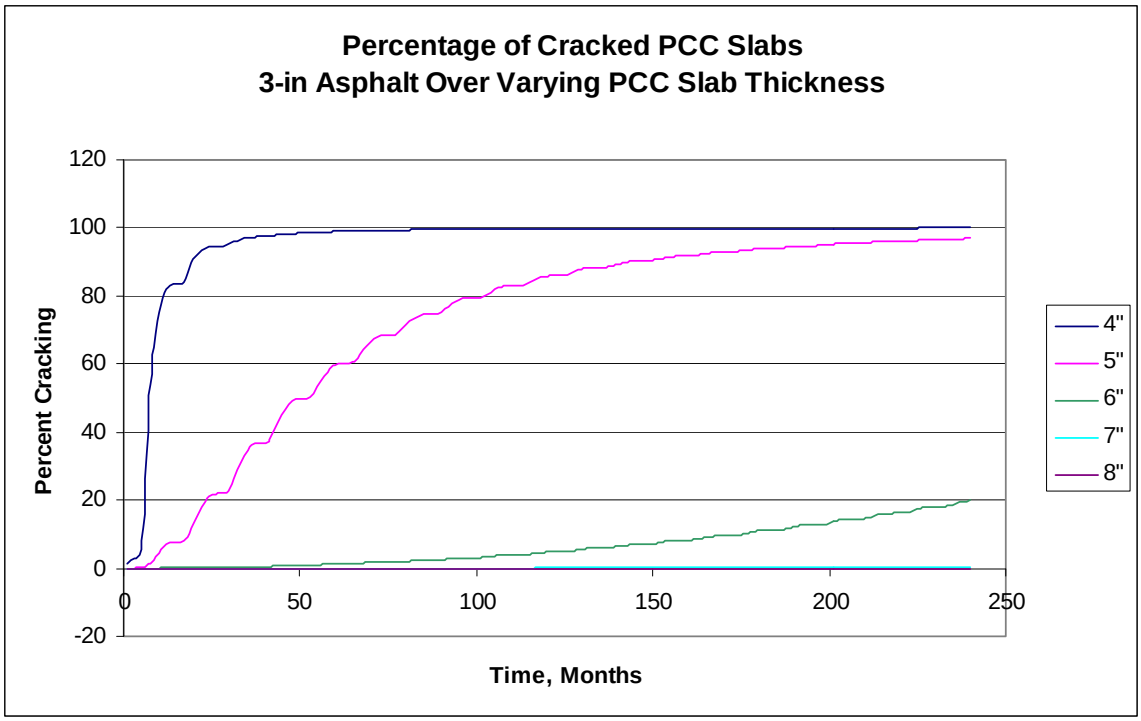

Figure 4.2 - Effect of PCC thickness for an AC/PCC composite pavement with 3-in AC layer.

The results indicate that the predicted pavement performance of an AC/PCC composite structure is very sensitive to the thickness of the PCC layer. It is also noted that a 9-in AC/PCC composite pavement with a 7-in PCC layer will support much more traffic, over 3000 AADTT, than a 9-in AC/PCC composite structure with a 6-in PCC layer.

4.2.2 Slab Width and Joint Spacing

The effect of slab width and joint spacing were examined, with the results listed in Tables 4.9 and 4.10.

Table 4.9 - Effect of Joint Spacing on Predicted Pavement Performance

Slab Length	% Cracking AC/PCC Pavement	% Cracking PCC Pavement
12'	0.0	0.8
15'	20.0	20.0
17'	68.1	75.3
19'	91.1	98.4

The predicted percentage of cracked slabs increased as the joint spacing, or slab length, increased. As joint spacing increased, the predictions for the composite structure were slightly less than the rigid structure. Both structures had a dramatic increase in cracking as joint spacing increased. As joint spacing increased two feet from 15 feet to 17 feet, predicted cracking increased from 20% to 68.1% (AC/PCC) and from 20% to 75.3% (PCC).

Table 4.10 - Effect of Slab Width on Predicted Pavement Performance

Slab Width	% Cracking AC/PCC Pavement	% Cracking PCC Pavement
12'	20.0	20.0
12.5'	2.3	3.0
13'	0.1	0.3
13.5	0.1	0.3
14'	0.1	0.3

The effect of slab width was essentially the same for the composite and rigid structures, with the composite structure predicted to exhibit slightly less cracking than the rigid structure. As width of the slab increased, the predicted percentage of cracked slabs decreased. This was expected, as a wheel load located farther from the edge (which is the

case for a widened slab) produces less tensile stress than the same load located at the slab edge.

4.2.3 Properties of Base and Subgrade

The MEPDG permits accounting for seasonal variation in properties of unbound materials by adjustment of the resilient moduli for each design period (month) [29]. The user has two options:

- Provide the resilient modulus for each design period or
- Provide resilient modulus for the optimum moisture content.

If the second option is selected, the Enhanced Integrated Climatic Model incorporated into the MEPDG software predicts seasonal variation in the moisture content of the unbound layers [13]. Then, the MEPDG software adjusts the moduli for the other moisture conditions using the following model [30, 31]:

$$M_R = 10^{a + \frac{b-a}{1+EXP(\beta + k_S \cdot (S - S_0))}} M_{Ropt}$$

where

M_R = resilient modulus at any degree of saturation;

S = degree of saturation while testing the material;

M_{Ropt} = resilient modulus at optimum water content and maximum dry density;

S_0 = degree of saturation at optimum water content;

a = minimum of $log\left(\frac{M_R}{M_{Ropt}}\right)$;

b = maximum of $log\left(\frac{M_R}{M_{Ropt}}\right)$;

β = location parameter, obtained as a function of a and b;

k_S = regression parameter.

For fine-grained materials, the Guide recommends the following model parameters:

a = -0.5934, b=0.4, β = -0.3944, k_S = 6.1324.

Figure 4.3 presents the correction factor for the moisture condition for the various degrees of saturation. One can observe that increase in moisture content decreases resilient modulus.

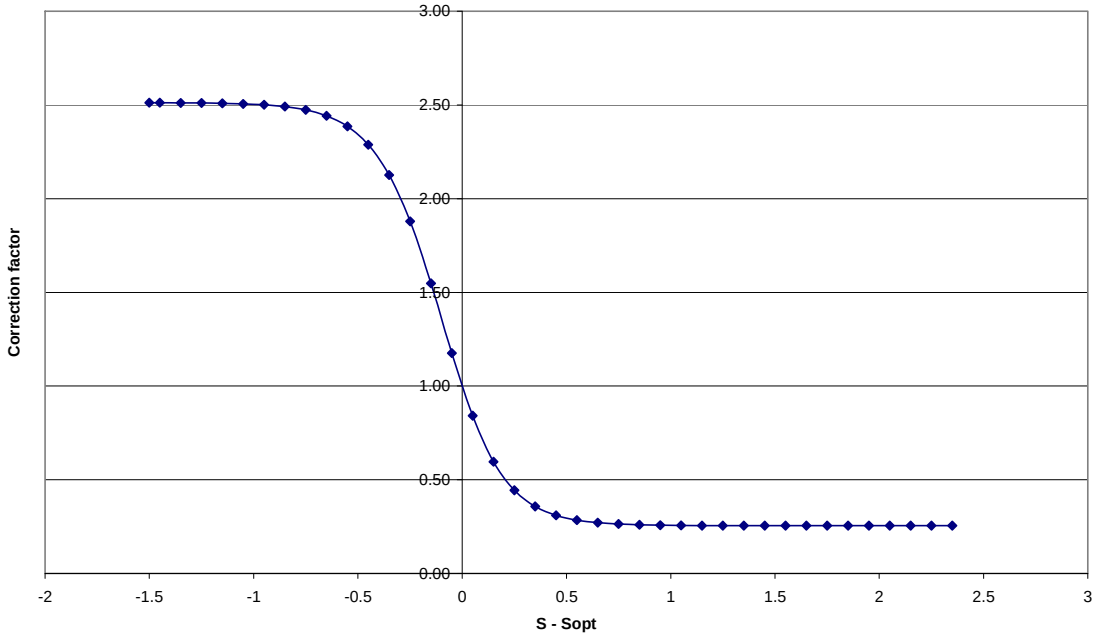

Figure 4.3 - Correction factor as a function of the degree of saturation.

The effect of the base properties on several modeled parameters was examined. Two base layers were considered with default resilient modulus values: A-1-a and A-3. Additionally, an A-3 base was modified by adjusting the resilient modulus value from 16,000 psi to 40,000 psi, which is the default value used by the EICM for an A-1-a base layer. Table 4.11 shows the default gradation values used by the MEPDG for the A-1-a and A-3 base materials.

Table 4.11 - MEPDG Default Gradation Values for A-1-a and A-3 Base Layers

Sieve	Percent Passing	
	A-1-a	A-3
#200	8.7	5.2
#80	12.9	33.0
#40	20.0	76.8
#10	33.8	94.3
#4	44.7	95.3
3/8"	57.2	96.6
1/2"	63.1	97.1
3/4"	72.7	98.0
1"	78.8	98.6
1 1/2"	85.8	99.2
2"	91.6	99.7
3 1/2"	97.6	99.9

Plotted in Figure 4.4 is the coefficient of subgrade reaction for the three different layers over the time period of one year, from January to December.

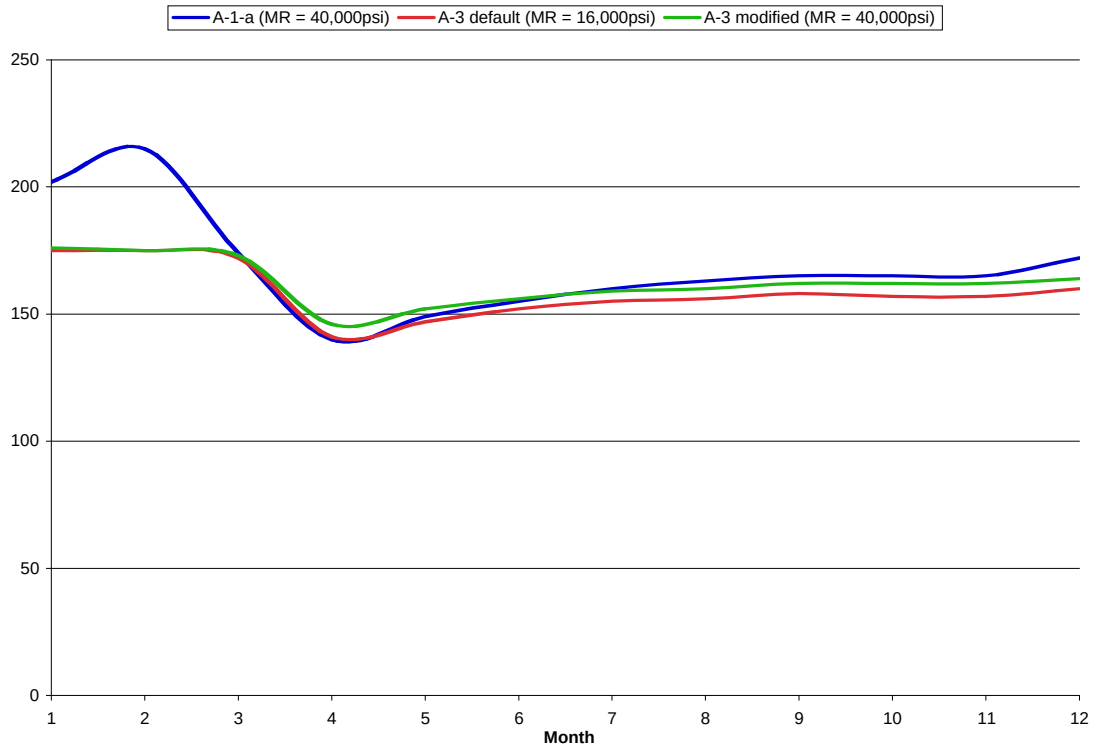

Figure 4.4 - Coefficient of subgrade reaction for three base layers: A-1-a, A-3, and A-3 (modified).

Figure 4.5 represents the modeled resilient modulus for the three base layers under consideration over the time period of one year, from January to December.

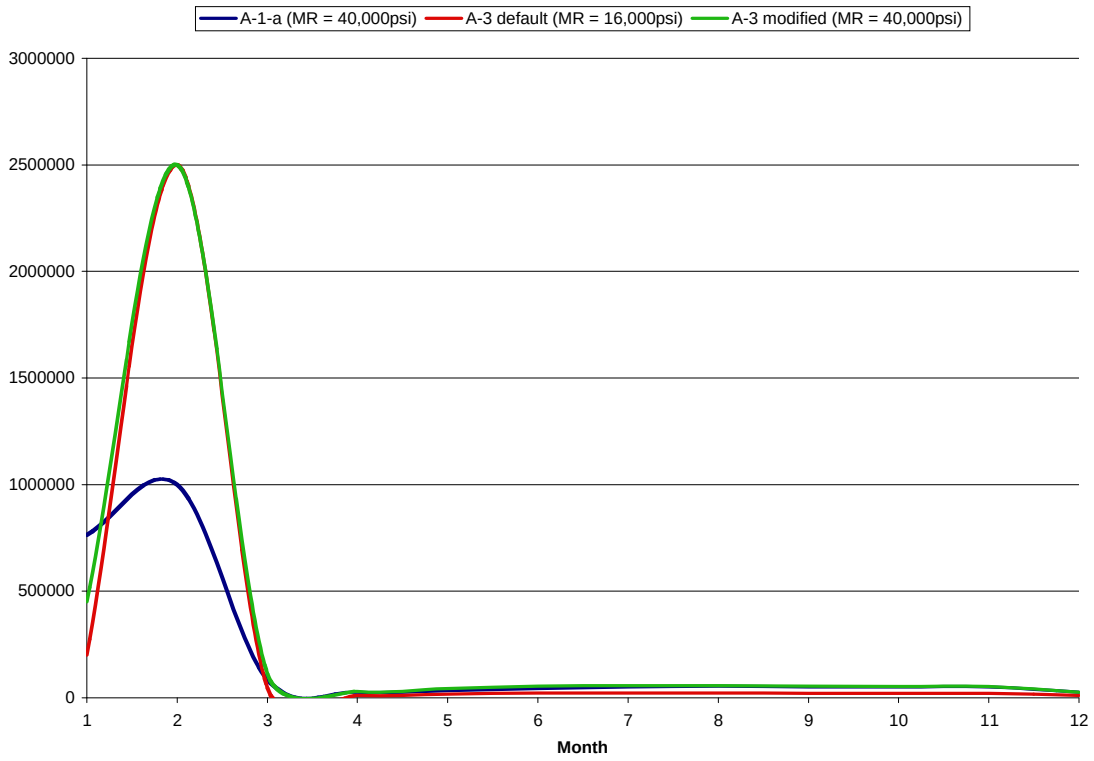

Figure 4.5 - Resilient modulus for three base layers: A-1-a, A-3, and A-3 (modified).

Figures 4.4 and 4.5 demonstrate that the gradation of the base layer has an equal or greater effect on the modeled resilient modulus in comparison to the input value for resilient modulus at optimum moisture content.

As a result, Figure 4.6 demonstrates that gradation affects predicted cracking in the PCC layer more than the resilient modulus at optimum moisture content.

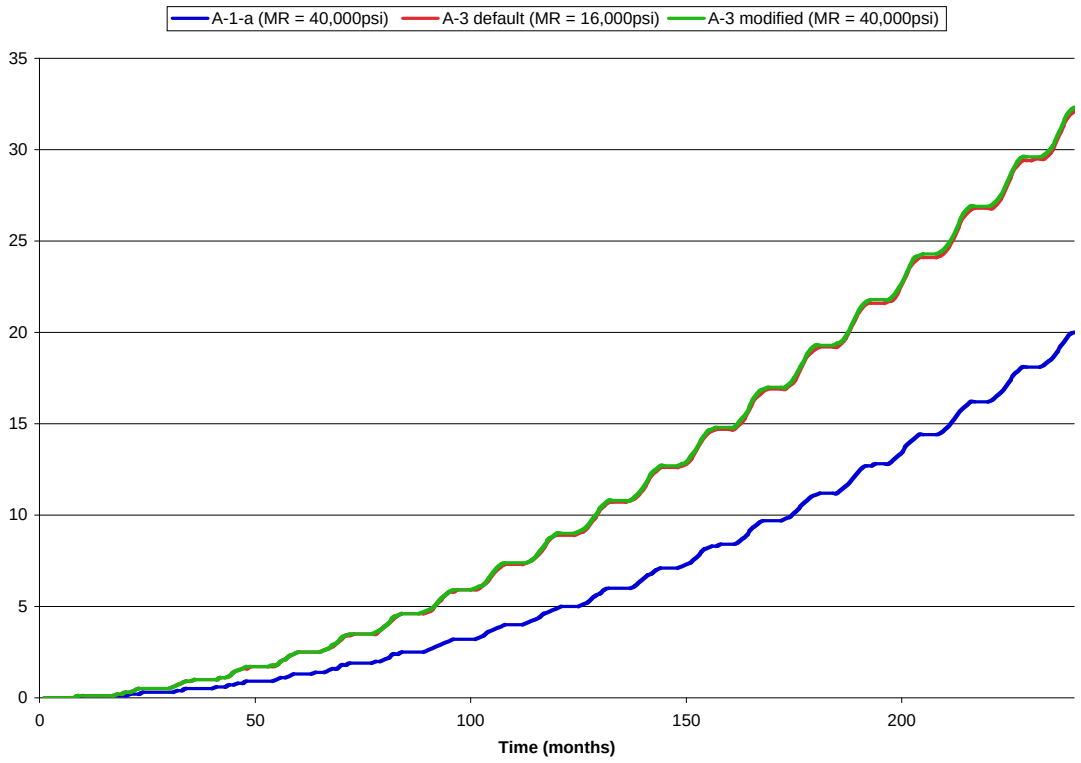

Figure 4.6 - Effect of base layer material for an AC/PCC composite pavement.

Chapter 5 – Conclusions

While many aspects of the MEPDG modeling and design inputs have been the subject of a great deal of research, very little of the MEPDG dealing with climate and its impact on pavement performance prediction has been a subject of an in-depth analysis in the past. The dual focus of this report was an analysis of the effect of climate on MEPDG predictions, and the thermal characteristics of a composite pavement system and the modeling of these characteristics relative to measured environmental conditions.

First, a comprehensive sensitivity study of the effect of climate on the MEPDG performance prediction was conducted. Pavement performance was simulated at more than 600 locations across the US using the climatic database data supplied by the MEPDG.

It was found that the environment has a significant impact on predicted pavement performance. A pavement may perform exceptionally good or bad, depending upon where it is located and the conditions it subjected to. A limited analysis was performed comparing trends by region. These trends were found to be reasonable. Nevertheless, differences in predicted pavement performance among stations with similar environmental conditions were greater than expected. This illustrates the importance of high-quality climatic data to obtain reliable pavement performance predictions. Therefore, there is a need for both a vigorous data check and data cleaning in the climatic database.

The quality of the climatic data in the database in non-uniform, and the MEPDG allows stations with low-quality data to be used. Although the MEPDG does not permit stations with missing data to be used alone, these stations can be used when creating a virtual weather station through interpolation. The report demonstrated that the use of incomplete weather stations may only decrease the quality of predictions. Thus, it is recommended

that all stations with incomplete data be removed from the database.

While the database verification may take substantial time and resources, a simple, practical approach for the evaluation of data quality is suggested. A pavement structure is tested using climatic data from one station; the same structure is tested using a virtual weather station, which incorporates data from nearby stations. If these tests yield significantly different results, one of the following may be the case: a nearby station has low-quality data, or, the station used in the stand-alone test has low-quality data. This test will hold true for locations where there are no significant changes in climate or elevation. This test may not be reliable in mountainous regions.

If data quality is improved and uniform for each testing station, MEPDG performance would likely improve, and produce more reliable results. Data improvement will be a result of: cleaning data, and making the data from each station uniform and of high quality; and having more data, to eliminate year-to-year variations.

The other primary focus of this study examined measured and modeled temperature distributions in the PCC layer of JPCP and AC-over-PCC pavement structures. Hourly temperature data recorded from AC/PCC composite and JPCP cells located at MnROAD were collected and filtered to remove suspect measurements. This data was then used to investigate the effects of climate on these two pavement systems and validate expectations as an initial check of data quality. Measured data indicated diurnal AC surface temperatures were markedly higher than those of a PCC surface due to albedo. Despite the overall greater temperature difference through the full depth of the AC/PCC structure, temperature records showed the thermal gradient in a PCC layer was significantly less if an AC overlay was present. This effect is thought to contribute to the longevity and improved performance of the underlying PCC structure. EICM simulations were also found to reproduce the insulating effect of an AC overlay observed in the MnROAD data for composite test cells.

Furthermore, the research summarized in this report examined the sensitivity of the EICM and MEPDG to thermal conductivity input values for the AC and PCC layers. It was found that these parameters significantly influenced predicted pavement performance for MEPDG simulations, and this discovery led to further investigation of the influence of thermal conductivity on EICM predictions for thermal gradients through a simulated pavement system. A quantitative comparison of modeled and measured temperature data was conducted. The EICM simulations produced temperature distributions smaller than the measured distributions when the MEPDG default thermal conductivity value of PCC, k =1.25 BTU / hr-ft-°F, value was used. Several PCC thermal conductivity values were tested; the highest agreement between the measured and modeled data for a 6-in thick MnROAD test section occurred with a PCC thermal conductivity of 0.94 BTU / hr-ft-°F.

The authors note that adjustments to the MEPDG thermal property inputs in routine design should only be done with care. Solo improvement in prediction of the temperature distribution in the pavement structure does not necessarily lead to improvement in pavement performance predictions if the performance prediction models had been calibrated for the MEPDG default material thermal properties. Therefore, it is important to make evaluation of the MEPDG material thermal properties a part of a MEPDG local calibration process.

Finally, this thesis concludes that the environmental and material thermal property inputs should be considered with equal importance as traffic, design features, and non-thermal material properties.

Bibliography

[1] Yoder, E. J., and M. W. Witczak. *Principles of Pavement Design.* John Wiley and Sons, Inc., New York, 1975.

[2] Oh, J., D. Ryu, E. G. Fernando, and R.L. Lytton. Estimation of Expected Moisture Contents for Pavements by Soil and Water Characteristics, In *Transportation Research Record: Journal of the Transportation Research Board*, No. 1967, Transportation Research Board of the National Academies, Washington, D.C., 2006, pp. 135-147.

[3] *Guide for Mechanistic-Empirical Design of New and Rehabilitated Structures.* NCHRP Report 1-37A. TRB, National Research Council, Washington, D. C., 2004, Part 2, Ch.3

[4] Mamlouk, M. S., and J. P. Zaniewski. *Materials for Civil and Construction Engineers, 2nd Edition,* Pearson Education Company, Inc., Upper Saddle River, New Jersey, 2006.

[5] Herb, W., R. Velasquez, H. Stefan, M. Marasteanu, and T. Clyne. Simulation and Characterization of Asphalt Pavement Temperatures. *Road Materials and Pavement Design*, Vol. 10/1, pp. 233-247, 2009.

[6] Yu, H.T., K. D. Smith, M. I. Darter, J. Jiang, and L. Khazanovich. *Performance of Concrete Pavements*, Volume III: Improving Concrete Pavement Performance. Report FHWA-RD-95-111. FHWA, U.S. Departmentof Transportation, 1998.

[7] Ruiz Ruiz, J. M., A. G. Miron, G. K. Chang, R. O. Rasmussen, and Q. Xu. Use of Slab Curvature and ProVAL to Identify the Cause of Premature Distresses. In *Transportation Research Record: Journal of the Transportation Research Board*, No. 2068, Transportation Research Board of the National Academies, Washington, D.C., 2008, pp. 87-96.

[8] Selezevna, O. I., Y. J. Jiang, G. Larson, and T. Puzin. *LTPP Computed Parameter: Frost Penetration.* Publication FHWA-HRT-08-057. FHWA, U.S. Department of Transportation, 2008

[9] *AASHTO Guide for Design of Pavement Structures.* AASHTO, Washington, D.C., 1993

[10] ARA, Inc., ERES Consultants Division. *Guide for Mechanistic-Empirical Design of New and Rehabilitated Pavement Structures.* Final report, NCHRP Project 1-37A. Transportation Research Board of the National Academies. Washington, D.C., 2004. http://www.trb.org/mepdg/guide.htm

[11] *Mechanistic–Empirical Pavement Design Guide, Interim Edition:A Manual of Practice.* AASHTO, Washington, D.C., 2008.

[12] Lytton, R. L., D. E. Pufahl, C. H. Michalak, H. S. Lang, and B. J. Dempsey. *An Integrated Model of the Climatic Effects on Pavements.* Publication FHWA-RD-90-033. FHWA, U.S. Department of Transportation, 1989.

[13] Larson, G., and B. J. Dempsey. *Enhanced Integrated Climatic Model. Version 2.0.* Final report. Department of Civil Engineering, University of Illinois at Urbana–Champaign, 1997.

[14] Hall, K. D., and S. Beam. Estimating the Sensitivity of Design Input Variables for Rigid Pavement Analysis with a Mechanistic-Empirical Design Guide. In *Transportation Research Record: Journal of the Transportation Research Board*, No. 1919, Transportation Research Board of the National Academies, Washington, D.C., 2005, pp. 65-73.

[15] Graves, R. C., and K. C. Mahboub. Pilot Study in Sampling-Based Sensitivity Analysis of NCHRP Design Guide for Flexible Pavements. In *Transportation Research Record: Journal of the Transportation Research Board*, No. 1947, Transportation Research Board of the National Academies, Washington, D.C., 2006, pp. 123-135.

[16] Kannekanti, V., and J. Harvey. Sensitivity Analysis of 2002 Design Guide Distress Prediction Models for Jointed Plain Concrete Pavement. Report No. UCPRC-DG-2006-01, California Department of Transportation, University of California, Davis and Berkeley. September 2006.

[17] Khazanovich, L., I. Yut, S. Husein, C. Turgeon, and T. R. Burnham. Adaptation of *Mechanistic–Empirical Pavement Design Guide* for Design of Minnesota Low-Volume Portland Cement Concrete Pavements. In *Transportation Research Record: Journal of the Transportation Research Board, No. 2087*, Transportation Research Board of the National Academies, Washington, D.C., 2008, pp. 57–67.

[18] Hiller, J. E., and J. R. Roesler. Determination of Critical Concrete Pavement Fatigue Damage Locations Using Influence Lines. *Journal of Transportation Engineering*, Vol. 131, No. 8, July–August 2005, pp. 599–607.

[19] Zapata, C. E., and W. N. Houston. *Calibration and Validation of the Enhanced Integrated Climatic Model for Pavement Design.* NCHRP Report No. 602, National Cooperative Highway Research Program, Transportation Research Board of the National Academies, Washington, D.C., 2008.

[20] Birgisson, B., J. Ovik, and D. E. Newcomb. Analytical Predictions of Seasonal Variations in Flexible Pavements. In *Transportation Research Record: Journal of the Transportation Research Board*, No. 1730, Transportation Research Board of the National Academies, Washington, D.C., 2000, pp. 81-90.

[21] Zaghoul, S., A. Ayed, A. Abd El Halim, N. Vitillo, and R. Sauber. Investigations of the Environmental and Traffic Impacts on Mechanistic-Empirical Pavement Design Guide Predictions. In *Transportation Research Record: Journal of the Transportation Research Board*, No. 1967, Transportation Research Board of the National Academies, Washington, D.C., 2006, pp. 148-159.

[22] *NCHRP Research Results Digest No. 307: Independent Review of the Mechanistic–Empirical Design Guide and Software.* Transportation Research Board of the National Academies, Washington, D.C., 2006.

[23] UK Meteorological Office, *Met Office: Climate Averages.* Retrieved from: http: //www.metoffice.gov.uk/climate/uk/averages, Accessed 15 July 2009

[24] Marasteanu, M., R. Velasquez, W. Herb, J. Tweet, M. Turos, M. Watson, H. G. Stefan. *Determination of Optimum Time for the Application of Surface Treatments to Asphalt Concrete Pavements - Phase II*. MnDOT Report No. MN/RC 2008-16.

[25] Nishizawa, T., S. Shimeno, A. Komatsubara, and M. Koyanagawa. Temperature Gradient of Concrete Pavement Slab Overlaid with Asphalt Surface Course. In *Transportation Research Record: Journal of the Transportation Research Board*, No. 1730, Transportation Research Board of the National Academies, Washington, D.C., 2000, pp. 25-33.

[26] Minnesota Department of Transportation, Current (2010) Test Sections, http://www.dot.state.mn.us/mnroad/testsections/mainline.html, Accessed 30 July 2010.

[27] Tompkins, D. and L. Khazanovich. *MnROAD Lessons Learned*. Final Report MN/RC-2007-06. Minnesota Department of Transportation, 2007.

[28] Barnes, R. *MnROAD Data Mining, Evaluation and Quantification – Phase I*. Draft Final Report. Minnesota Department of Transportation, 2009.

[29] Khazanovich, L., C. Celauro, B. Chadbourn, J. Zollars, and S. Dai. Evaluation of Subgrade Resilient Modulus Predictive Model for Use in Mechanistic-Empirical Pavement Design Guide. *Transportation Research Record: Journal of the Transportation Research Board*, No. 1947, Transportation Research Board of the National Academies, Washington, D.C., 2006, pp. 155-166.

[30] Witczak, M. W., D. Andrei and W. N. Houston. *Resilient Modulus as Function of Soil Moisture – Summary of Predictive Models*. Development of the 2002 Guide for the Development of New and Rehabilitated Pavement Structures, NCHRP 1-37 A, Inter Team Technical Report (Seasonal 1), 2000.

[31] Witczak, M. W., W. N. Houston, C. E. Zapata, C. Richter, G. Larson and K. Walsh. *Improvement of the Integrated Climatic Model for Moisture Content Predictions.* Development of the 2002 Guide for the Development of New and Rehabilitated Pavement Structures, NCHRP 1-37 A, Inter Team Technical Report (Seasonal 4), June 2000.